Biosensors and Bioelectronics 141 (2019) 111447

Contents lists available at ScienceDirect

Biosensors and Bioelectronics

journal homepage: www.elsevier.com/locate/bios

Recent advances of molecularly imprinted polymer-based sensors in the detection of food safety hazard factors

Yunrui Cao[a], Tingyu Feng[a], Jie Xu[a,*], Changhu Xue[a,b,**]

[a] College of Food Science and Engineering, Ocean University of China, Qingdao, 266003, PR China
[b] Qingdao National Laboratory for Marine Science and Technology, Qingdao, 266235, PR China

ARTICLE INFO

Keywords:
Food safety hazard factors
Molecularly imprinted polymers
Sensors
Detection

ABSTRACT

With increasing economic globalization, food safety is becoming the most serious concern in the food production and distribution system. Food safety hazard factors (FSHFs) can be categorized into chemical hazards, biological hazards and physical hazards, with the detection of the former two having fascinated interdisciplinary research areas spanning chemistry, material science and biological science. Molecularly imprinted polymer (MIP) -based sensors overcome many limitations of traditional detection methods and provide opportunities for efficient, sensitive and low-cost detection using smart miniaturized equipment. With highly specific molecular recognition capacity and high stability in harsh chemical and physical conditions, MIPs have been used in sensing platforms such as electrochemical, optical and mass-sensitive sensors as promising alternatives to bio-receptors for food analysis. In this systemic review, we summarize recent advances of MIPs and MIP-based sensors, such as popular monomers, usual polymerization strategies, fresh modification materials and advanced sensing mechanisms. The applications of MIP-based sensors in FSHF detection are discussed according to sensing mechanisms, including electrochemistry, optics and mass-sensitivity. Finally, future perspectives and challenges are discussed.

1. Introduction

Food safety has posed as a worldwide challenge for human health, especially in developing countries (Lv et al., 2018). Chemical hazards and biological hazards are the main food safety hazard factors (FSHFs) that can cause food intoxication and foodborne illness. To facilitate supervision and traceability, FSHFs are classified according to their sources. In Fig. 1, we provide an overview of FSHFs at all stages of the food chain. Chemical hazards mainly include natural toxins contained by raw-food materials (e.g. histamine, saxitoxin), residues of pesticides, fishery and veterinary drugs during farming (e.g. dimethoate, chloramphenicol), environmental contaminants from soil and water (e.g. tributyltin), abused additives (e.g. Sudan II, melamine), as well as the contaminants from processing and packaging (e.g. acrylamide, bisphenol A). Biological hazards include various contaminations caused by fungi, bacteria and viruses, such as aflatoxin, *Escherichia coli* and hepatitis A virus. Monitoring the levels of FSHFs not only confirms to food security, but also provides guiding technical data on agriculture production, food processing and food safety risk analysis and control (Motarjemi and Fritz, 1999).

A wide range of well-developed techniques have been employed for FSHF detection, such as high-performance liquid chromatography (HPLC), gas chromatography (GC), high-performance liquid chromatography-mass spectrometer (HPLC-MS), gas chromatography-mass spectrometer (GC-MS), and nuclear magnetic resonance (NMR) (Hong et al., 2017). However, these techniques have inherent limitations, such as long detection time, high dependence on sample preparation techniques and expensive instruments, which limit their applications. On the other hand, biosensors have shown great potential in the field of food analysis because of their low-cost, portability, ease of fabrication and operation (Maduraiveeran et al., 2018; Wu et al., 2018). Depending on the transducer, biosensors can be classified into electrochemical, optical and other sensors (Wackerlig and Lieberzeit, 2015), among which electrochemical and optical sensors are especially widely used in the detection of FSHFs. Aptamers (Barreda-García et al., 2018; Wang et al., 2017b; Wu et al., 2015; Yan et al., 2016), enzymes (Liu et al., 2017a; Song et al., 2018) and other natural receptors (Kaushal et al., 2019; Wang et al., 2019a) have been widely studied for the application on sensing platforms. Recently, artificial synthetic receptors have also received extensive attention, and molecularly imprinted polymers (MIPs) have become a competitive alternative.

MIPs possess unique properties that offer significant advantages for

* Corresponding author. College of Food Science and Engineering, Ocean University of China, No.5 Yushan Road, Qingdao, Shandong Province, 266003, PR China.
** Corresponding author. College of Food Science and Engineering, Ocean University of China, No.5 Yushan Road, Qingdao, Shandong Province, 266003, PR China.
E-mail addresses: 21180711002@stu.ouc.edu.cn (Y. Cao), ftyxy1986@163.com (T. Feng), xujie9@ouc.edu.cn (J. Xu), xuech@ouc.edu.cn (C. Xue).

https://doi.org/10.1016/j.bios.2019.111447
Received 2 April 2019; Received in revised form 5 June 2019; Accepted 17 June 2019
Available online 19 June 2019
0956-5663/

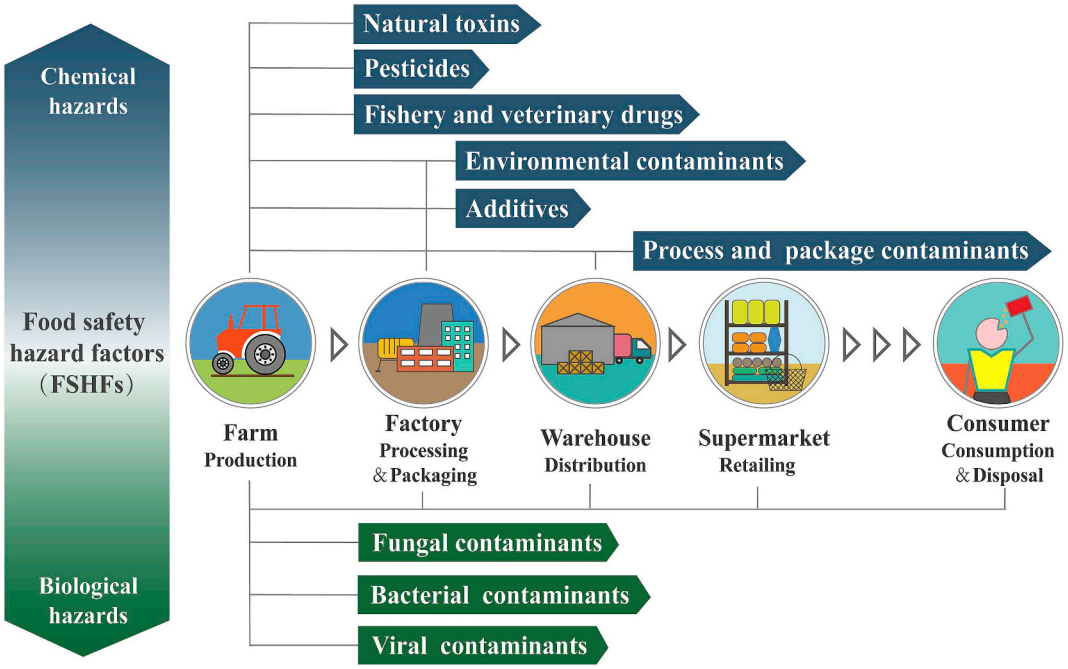

Fig. 1. Conceptual framework of food production and distribution system and the category of FSHFs.

FSHF analysis. With inherent molecular recognition abilities, MIPs can recognize not only small molecules but also various macromolecular targets, including proteins (Chunta et al., 2018; Magni et al., 2015), viruses (Altintas et al., 2015; Zhang et al., 2018; Liu et al., 2017c) and microorganisms (Poller et al., 2017), essentially covering all categories of FSHFs. At the same time, studies have consistently shown that MIPs have high efficiency for the retention of analytes and improved selectivity (Ashley et al., 2017). In addition, compared with natural receptors, MIPs have higher stability in harsh chemical and physical conditions and relatively simple sample preparations hence lower cost, which enables MIPs great potential in practical applications (Ashley et al., 2017; Eersels et al., 2016).

MIPs are based on advanced polymerization techniques and have been applied in various sensing platforms as electrochemical (Beloglazova et al., 2018; Guo et al., 2017), optical (Wu et al., 2017b; Yılmaz et al., 2017) and other (Lin et al., 2018; Qian et al., 2016) sensors. By combining the advantages of MIPs, nanomaterials and advanced micromachining technology, MIP-based sensors make it possible to fabricate low-cost, convenient, efficient and portable devices with ideal selectivity and sensitivity for FSHF detection. It is expected that MIP-based sensors will take their place in sensor markets in the near future.

In this review, we summarize the progresses in the development of MIP-based sensors for FSHF detection in the past 5 years. Firstly, current MIPs in biosensor are reviewed. Secondly, the type of MIP-based sensors applied to FSHF detection are introduced and discussed in detail. Thirdly, the sensing applications of electrochemical, optical and mass-sensitive MIP-based sensors in FSHF detection are highlighted. Finally, present challenges and future research directions are discussed.

2. MIPs in biosensors

MIPs are synthesized by co-polymerization of functional monomers and cross-linkers in the presence of templates. After removing templates, cavities matching in size, shape and groups with templates are created, which provides MIPs the ability to recognized template molecules (Fig. 2A). Based on this general principle, different polymerization strategies and monomer combinations are developed for different applications. For biosensor fabrication, MIPs are always deposited as thin films. Therefore, precipitation polymerization and electropolymerization are frequently-used methods (Table 1). Photo-polymerization is also a potential method (Huang et al., 2018; Sergeyeva et al., 2017; Yang and Park, 2016).

Apart from steric factors, the specific interaction between functional monomers and targets provides MIPs increased affinity and selectivity to the analyte (Cieplak and Kutner, 2016). Functional monomers containing acidic or basic groups are often used, which are capable of forming covalent bonds, hydrogen bonds and other interactions with analyte molecules inside imprinted cavities. For the detection of FSHFs, methacrylic acid (MAA) and 3-aminopropyl-triethoxysilane (APTES) are the most popular functional monomers (Table 1). These functional monomers are always co-polymerized with cross-linkers, such as ethylene glycol dimethacrylate (EGDMA) and tetraethyl orthosilicate (TEOS). Besides, *o*-phenylenediamine, pyrrole, dopamine, *o*-aminophenol and p-aminothiophenol have shown great properties as functional monomers because of their ability of electropolymerization without cross-linker. With the development of statistics and computer technology, combinatorial and computational design have been used to select the most appropriate functional monomer and template: monomer ratio for polymerization (Sergeyeva et al., 2017; Uzun and Turner, 2016).

MIPs in biosensors can not only separate analyst from food samples to enhance selectivity but also aggregate target materials around the sensing surface to improve sensitivity. However, recent studies have also identified several disadvantages of MIPs, such as residue of template molecules, limited selectivity and finite mass-transport ability (Uzun and Turner, 2016). The shape memory conducting hydrogel (Wei et al., 2019) was prepared as MIP films to remove targets more thoroughly. To further improve the detection properties of MIPs in biosensors, novel structural systems have been applied (Fig. 2B). Thin MIP film can be polymerized on the surface of sensing platform to enhance the mass transport (Capoferri et al., 2017; Elshafey and Radi, 2018; Turco et al., 2015), hence the respond time can be shortened efficiently. Nanomaterials have been applied by modifying the surface of sensing platform or carrying MIP films (Wang et al., 2017a; Yin et al., 2018a), which can not only expand effective sensing area but also optimize biosensors' performances, such as reutilization, electrical conductivity and portability. Carbon nanotubes (CNTs) (Amatatongchai et al., 2018;

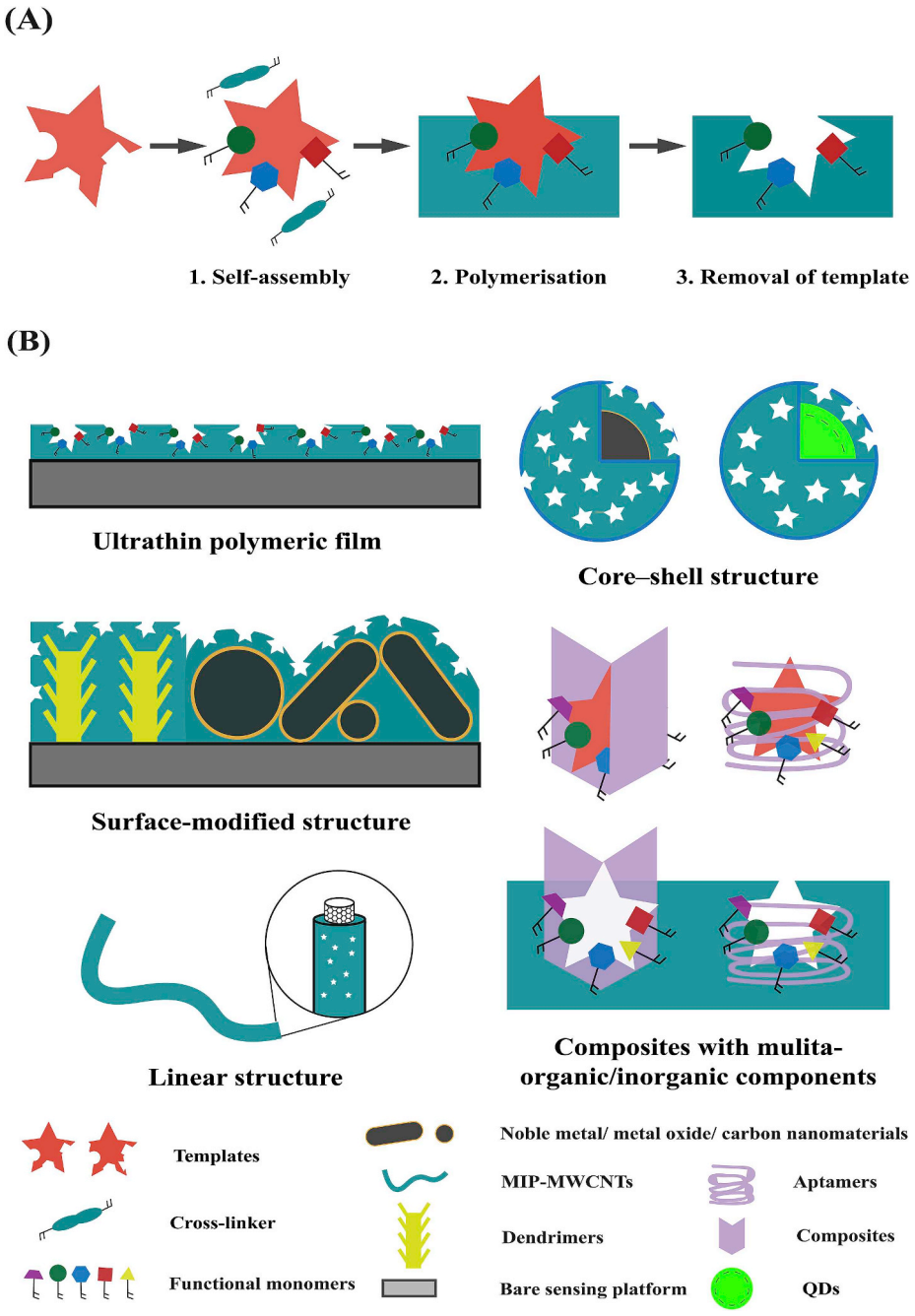

Fig. 2. (A) Schematic of molecular imprinting; (B) Common configuration status of MIPs in biosensors.

Bai et al., 2017), noble metal nanoparticles (Fan et al., 2018; Wang et al., 2017a), nanoporous metals (Li et al., 2015a, 2015c) and metal-organic frameworks (MOFs) (Stassen et al., 2017; Zhang et al., 2018) are popular nanomaterials with structural functions. F_3O_4 magnetic nanoparticles (Li and Wang, 2013; Li et al., 2017a), magnetic graphene (Jia et al., 2019) are synthesized to assemble recyclable magnetic MIP composites. Meanwhile, multiple recognition combing MIPs and other identifying materials, such as aptamer (Ensafi et al., 2018; Rezaei et al., 2016) and calixarenes (Li et al., 2016a, 2016b), have been designed to increase the selectivity of targets. The synergies between MIPs and these functional materials have effectively improved the sensitivity and selectivity of FSHF detection.

3. Types for MIP-based sensors for the detection of FSHFs

For the detection of FSHFs, MIP-based sensors have shown great potential because of their low-cost, miniaturization and ease of operation (Maduraiveeran et al., 2018; Wu et al., 2018). Recent literature reveal that electrochemical and optical sensing are the most commonly utilized analytical technique to be combined with MIPs. Meanwhile, attempts also have been made in other sensing techniques, such as quartz crystal microbalance (QCM). Fig. 3 summarizes different MIP-based sensors and their principles.

Electrochemical sensors are detectors with electrochemical transducers which can transform the interaction of analytes with the receptors on the surface of an electrode into analytical signal (The'venot et al., 2001). Thereinto, three-electrode structure, including working, reference and counter electrodes, is the most classic system. Integrating

Table 1
Usually utilized functional monomers providing defined recognizing sites for FSHFs detection.

No.	Functional monomers	Testing FSHFs		Possible interactions with FSHFs	Polymerization	Cross-linker or co-monomer	Ref.
1	**Methacrylic acid**	**Natural toxins**	Histamine	Hydrogen bonds and electrostatic forces	UV photo-polymerization/ Precipitation polymerization	Cross-linker: acetonitrile/EGDMA/TRIM	Basozabal et al. (2014); Jiang et al. (2016); Mattsson et al. (2018)
		Pesticides	Atrazine	Hydrogen bonds	UV photo-polymerization	Cross-linker: EGDMA	Yang and Park (2016)
			Dinotefuran	Hydrogen bonds	Precipitation polymerization	Cross-linker: EGDMA	Abdel-Ghany et al. (2017)
			Metolcarb	Hydrogen bonds	One-step polymerization	Cross-linker: EGDMA	Fang et al. (2017)
			Bitertanol	Hydrogen bonds and π-π stacking	Precipitation polymerization	Cross-linker: TRIM	Cao et al. (2018)
			Methanephosphonic acid	Hydrogen bonds	UV photo-polymerization	Cross-linker: PEGDA	Huang et al. (2018)
			λ- cyhalothrin	–	Atom transfer radical polymerization	Co-monomer: AM Cross-linker: EGDMA	Li et al. (2018a)
			Cyfluthrin	Hydrogen bonds and ionic interaction	Precipitation polymerization	Co-monomer: APTES Cross-linker: EGDMA and TEOS	Li et al. (2018c)
			Carbofuran	Hydrogen bonds	Precipitation polymerization	Cross-linker: N,N′-methylene diacrylamide	Li et al. (2018b)
			Triazophos	–	Thermal polymerization	Cross-linker: TRIM	She and Wang (2019)
		Fishery and veterinary drugs	Ractopamine	–	Precipitation polymerization	Cross-linker: EGDMA	Yao et al. (2016)
			Enrofloxacin	Hydrogen bonds	Precipitation polymerization	Cross-linker: TRIM	Liu et al. (2017b)
			Sulfapyridine	–	Precipitation polymerization	Cross-linker: EGDMA	Liu et al. (2019)
			Benzimidazoles	–	Precipitation polymerization	Cross-linker: EGDMA	Cai et al. (2019)
			Sulfaguanidine	Hydrogen bonds	Thermal-polymerization	Cross-linker: EGDMA	Li et al. (2019a)
			Chloramphenicol	–	Precipitation polymerization	Cross-linker: divinylbenzene	(Jia et al., 2019)
		Environmental contaminants	2,4- dichlorophenol	Hydrogen bonds and π-π stacking	Precipitation polymerization	Cross-linker: EGDMA	El-Kosasy et al. (2018); Liang et al. (2017)
			Tributyltin	–	Mini-emulsion polymerization	Cross-linker: EGDMA	Sari et al. (2019)
		Additives	Melamine	–	Precipitation polymerization	Cross-linker: EGDMA	Shrivastav et al. (2015)
			Rhodamine 6G	Hydrogen bonds	Precipitation polymerization	Cross-linker: EGDMA	Li et al. (2019c)
			Caffeine	π-π stacking	Thermal-polymerization	Cross-linker: TRIM	Betlem et al. (2019)
		Process and package contaminants	Acrylamide	Hydrogen bonds	Precipitation polymerization	Cross-linker: EGDMA	Liu et al. (2018)
			3-monochloropropane-1,2-diol determination	Hydrogen bonds	Precipitation polymerization	Cross-linker: EGDMA	Fang et al. (2019)
1	**Methacrylic acid**	**Fungal contaminants**	Sterigmatocystin	Hydrogen bonds	Non-hydrolytic sol–gel process	Cross-linker: γ-methacryloxypropyltrimethoxysilane	Xu et al. (2016)
			Aflatoxins	–	Precipitation polymerization	Cross-linker: divinylbenzene-80	Chmangui et al. (2019)
		Bacterial contaminants	N-acyl-homoserine lactones (quorum signaling molecules of gram-negative bacteria)	Hydrogen bonds	Precipitation polymerization	Cross-linker: EGDMA	Habimana et al. (2018); Jiang et al. (2016)
2	**3-aminopropyl-triethoxysilane**	**Natural toxins**	Saxitoxin	Hydrogen bonds	Precipitation polymerization	Cross-linker: TEOS	Sun et al. (2018)
		Pesticides	Metolcarb	–	Precipitation polymerization	Cross-linker: TEOS	Qian et al. (2016)
			Cypermethrin	Hydrogen bonds and ionic interactions	Room-temperature reverse micro-emulsion polymerization	Cross-linker: TEOS	Xiao et al. (2016)
			Methamidophos or Omethoate	Hydrogen bonds	Precipitation polymerization	Cross-linker: TEOS	Shi et al. (2017)
			Acetamiprid	Hydrogen bonds and Van der Waals force	Sol-gel polymerization	Cross-liner: tetramethoxysilane	Shirani et al. (2019)
		Fishery and veterinary drugs	Diethylstilbestrol	Hydrogen bonds	Precipitation polymerization	Cross-linker: TEOS	Bai et al. (2017)
			Sulfadiazine	Hydrophobic effect	Precipitation polymerization	Cross-linker: TEOS	Ding et al. (2017)
			17β- estradiol	–	Precipitation polymerization	Cross-linker: TEOS	Xiao et al. (2017)
			Malachite green	Hydrogen bonds	Room-temperature reverse micro-emulsion polymerization	Cross-linker: TEOS	Wu et al. (2017a,2018)
		Additives	Melamine	Hydrogen bonds and covalent bonds	One-pot synthesis	Cross-linker: TEOS	Xu and Lu (2015)

(*continued on next page*)

Table 1 (*continued*)

No.	Functional monomers	Testing FSHFs		Possible interactions with FSHFs	Polymerization	Cross-linker or co-monomer	Ref.
		Process and package contaminants	Bisphenol A	Hydrogen bonds	Precipitation polymerization	Cross-linker: EGDMA	Dadkhah et al. (2016)
		Fungal contaminants	Patulin	Hydrogen bonds	Precipitation polymerization	Cross-linker: TEOS	Fang et al. (2016)
		Viral contaminants	Human norovirus	–	Precipitation polymerization	Cross-linker: TEOS	Sykora et al. (2015)
3	***o*-phenylenediamine**	**Pesticides**	Carbofuran	Hydrogen bonds	Electropolymerization	–	Li et al. (2016b); Amatatongchai et al. (2018)
			Alachlor	Hydrogen bonds	Electropolymerization	–	Elshafey and Radi (2018)
			Chlorpyrifos	Hydrogen bonds and π-π stacking	Electropolymerization	Co-monomer: *o*-Dihydroxybenzene	Roushani et al. (2018)
		Fishery and veterinary drugs	Metronidazole	Hydrogen bonds, electrostatic forces and van der Waals force	Electropolymerization	–	Li et al. (2015a, 2015c); Song et al. (2016)
			Salbutamol	Hydrogen bonds	Electropolymerization	–	Li et al. (2017b)
			Olaquindox	Hydrogen bonds and electrostatic interactions	Electropolymerization	–	Wang et al. (2017a)
			Nitrofurantoin	Hydrogen bonds and π-π stacking	Electropolymerization	Co-monomer: resorcinol	Dechtrirat et al. (2018)
			Clenbuterol	–	Electropolymerization	–	Jin et al. (2018)
		Environmental contaminants	Perfluorooctanesulfonate	–	Electropolymerization	–	Karimian et al. (2018)
		Additives	Sudan II	Hydrogen bonds and π-π stacking	Electropolymerization	–	Rezaei et al. (2016)
			Erythrosine	–	Electropolymerization	Co-monomer: m-dihydroxybenzene	Zhao et al. (2018)
			Tertiary butylhydroquinone	Hydrogen bonds	Electropolymerization	–	Yue et al. (2019)
4	**Acrylamide**	**Pesticides**	Cyphenothrin	–	Precipitation polymerization	Cross-inker: EGDMA	Ren and Chen (2015)
			Phoxim	–	Free radical polymerization	Cross-inker: EGDMA	Tan et al. (2015b)
			λ- cyhalothrin	Hydrogen bonds and covalent bonds	Two-step precipitation polymerization	Cross-inker: EGDMA	Wei et al. (2016)
			Dinotefuran	Hydrogen bonds	Precipitation polymerization	Cross-inker: EGDMA	Abdel-Ghany et al. (2017)
		Fishery and veterinary drugs	Malachite green	Hydrogen bonds	Precipitation polymerization	Cross-inker: EGDMA	Wu et al. (2017b)
			Oxytetracycline	Hydrogen bonds	UV photo-polymerization	Co-monomer: acrylic acid Cross-linker: N,N′-methylenebisacrylamide	Wang et al. (2019b)
4	**Acrylamide**	**Process and package contaminants**	Bisphenol A	π-π stacking and van der Waals force	Mini-emulsion polymerization	Co-monomer: vinyl imidazole Cross-inker: EGDMA	Üzek et al. (2019)
		Fungal contaminants	Aflatoxin B1	Hydrogen bonds, ionic interaction, Van der Waals and dipoledipole interactions	UV photo-polymerization	Cross-linker: tri (ethyleneglycol) dimethacrylate	Sergeyeva et al. (2017)

(*continued on next page*)

Table 1 (*continued*)

No.	Functional monomers	Testing FSHFs		Possible interactions with FSHFs	Polymerization	Cross-linker or co-monomer	Ref.
5	**Pyrrole**	**Pesticides**	Dimethoate	–	Electropolymerization	–	Capoferri et al. (2017)
			Chlorpyrifos	–	Thermal-polymerization	–	Capoferri et al. (2018)
		Fishery and veterinary drugs	Sulfadimethoxine	Electrostatic interactions	Electropolymerization	–	Turco et al. (2015)
		Additives	Tertiary butylhydroquinone	Hydrogen bonds and electrostatic interactions	Electropolymerization	–	Fan et al. (2018)
		Process and package contaminants	Bisphenol A	Hydrogen bonds and π-π stacking	Electropolymerization	–	Ensafi et al. (2018); Rao et al. (2018)
6	**Dopamine**	**Fishery and veterinary drugs**	Metronidazole	–	Electropolymerization	–	Liu et al. (2015)
			Sulfamethoxazole	Secondary reaction	Electropolymerization	–	Turco et al. (2018)
			Tetracycline	–	Electropolymerization	–	Rad and Azadbakht (2019)
		Additives	Sunset yellow	Hydrogen bonds, π-π stacking, and electrostatic interactions	Monomeric self-polymerization	–	Yin et al. (2018b)
			Amaranth	–	Self-polymerization	–	Li et al. (2019b)
			Cypermethrin	–	Electropolymerization	Co-monomer: resorcinol	Li et al. (2019d)
		Viral contaminants	Hepatitis A Virus	Hydrogen bonds and π-π stacking	Electropolymerization	–	Yang et al. (2017)
7	***o*-aminophenol**	**Pesticides**	Imidacloprid	Hydrogen bonds	Electropolymerization	–	Li et al. (2016a)
		Fishery and veterinary drugs	Virginiamycin	–	Electropolymerization	–	Li et al. (2017d)
			Lincomycin	Hydrogen bonds	Electropolymerization	–	Li et al. (2017c)
8	**Methyl acrylic acid**	**Pesticides**	Carbofuran	Hydrogen bonds	Precipitation polymerization	Cross-linker: EGMRA	Tan et al. (2015a)
		Fishery and veterinary drugs	Ciprofloxacin	Hydrogen bonds	Mini-emulsion polymerization	Co-monomer: HEMA Cross-linker: EGDMA	Okan et al. (2017)
			Erythromycin	Hydrogen bonds and covalent bonds	Mini-emulsion polymerization	Co-monomer: HEMA Cross-linker: EGDMA	Okan and Duman (2018)
9	**Tetraethyl orthosilicate**	**Process and package contaminants**	Bisphenol A	Hydrogen bonds	Non-covalent imprinting method	Cross-linker: APTES	Yin et al. (2018a)
		Fungal contaminants	Patulin	Hydrogen bonds	Precipitation polymerization	Cross-linker: APTES	Bagheri et al. (2018)
10	**P-aminothiophenol**	**Pesticides**	Chlorpyrifos	Hydrogen bonds	Electropolymerization	–	Sun et al. (2017)
		Process and package contaminants	4-nonylphenol	Hydrogen bonds	Electropolymerization	–	Zheng et al. (2018)

Ethylene glycol dimethacrylate (EGDMA), trimethylolpropane trimethacrylate (TRIM), poly (ethylene glycol) diacrylate (PEGDA), acrylamide (AM), 3-aminopropyl-triethoxysilane (APTES), tetraethoxysilane (TEOS), ethylene glycol maleic rosinate acrylate (EGMRA), 2-hydroxyethyl methacrylate (HEMA).

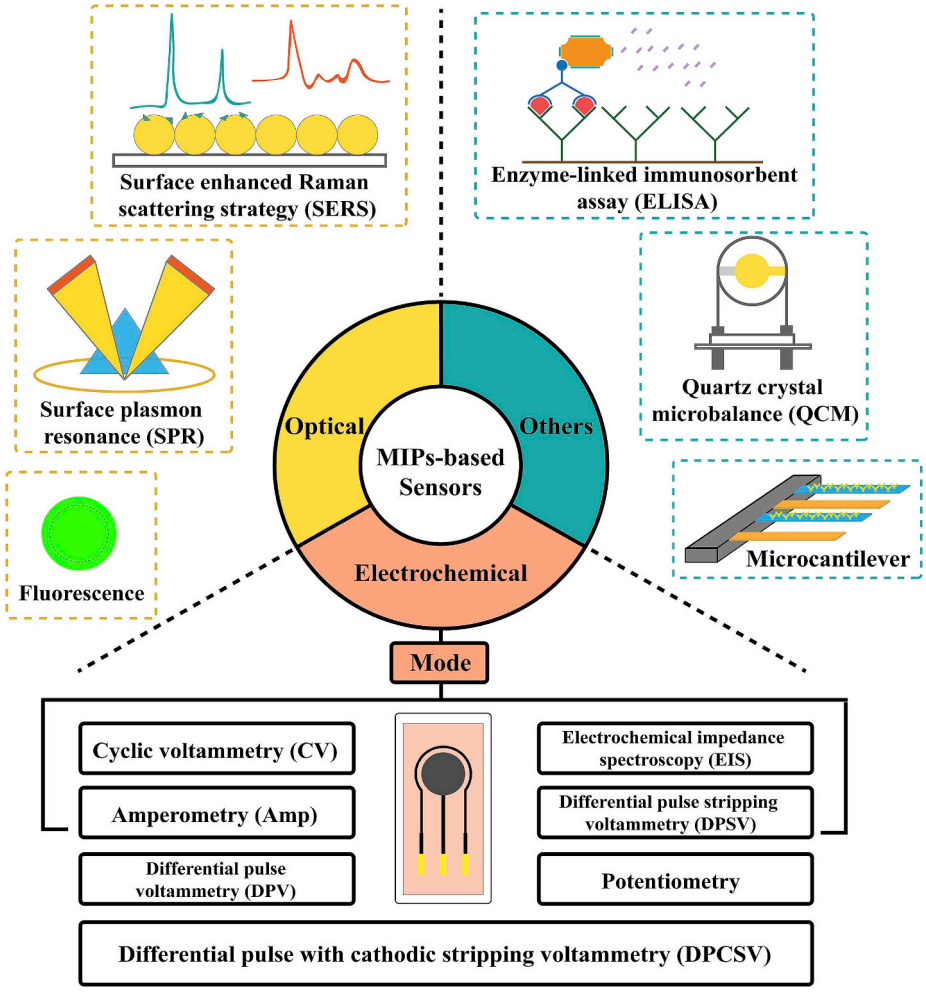

Fig. 3. Schematic representation of various types of MIP-based sensors.

the recognition elements, working electrodes play a crucial part in electrochemical sensors. Glassy carbon electrode (GCE) (Guo et al., 2017; Li et al., 2016a) and screen-printed carbon electrode (SPCE) (Dechtrirat et al., 2018) are popular electrodes. The combination of MIPs and target FHSFs can change the electric signals of electrodes, such as current, voltage, conductivity and capacitance or impedance (Ahmad et al., 2019). Different electroanalytical modes have been employed in electrochemical sensors, thereinto the current as the potential is varied (e.g. cyclic voltammetry, differential pulse voltammetry) and the current at a fixed voltage (e.g. amperometry) are the common measured properties in the electrochemical detection of FSHFs (Table 2). MIP-based electrochemical sensors are attractive because of their low cost and simplicity of production. Apart from GCE and Au electrode, screen-print electrodes (SPEs) are also combined with MIPs (Capoferri et al., 2018; Cardoso et al., 2019; Zamora-Gálvez et al., 2017). Laser-induced graphene technique (Cardoso et al., 2019) and dealloying (Song et al., 2016) are also applied to build electrodes with exquisite 3D structures. In addition, the mass transfer and conductivity of modified electrodes determine the performance of electrochemical sensors. Therefore, nanostructured coating and pre-assemblage of MIP-based nanomaterials are further used to develop modified electrodes. Before the synthesis of MIPs, conducting metal nanomaterials (Fan et al., 2018; Rao et al., 2018), carbon nanomaterials (Guo et al., 2017; Liu et al., 2015) or polymer (Shi et al., 2017) are deposited on the bare surface of an electrode to obtain better mechanical and electrical features. For the polymerization of MIPs, electropolymerization has become a popular method because of its rapid and handy process, as indicated in Table 1. On the other hand, multiwalled carbon nanotubes (MWCNTs) (Xu et al., 2018; Yang and Zhao, 2015; Yin et al., 2018b) and other various nanoparticles (Jiang et al., 2016; Zamora-Gálvez et al., 2017) can also serve as supporting materials for MIPs, and the obtained carriers@MIP are deposited on the electrode to construct the sensor.

Optical sensors are detectors measuring optical properties in materials and converting their changes into analytical signal, in which MIPs also play a role in identifying analytes and thus change the optical properties of materials (Ahmad et al., 2019). Different optical sensors combined with MIPs for the detection of FSHFs are summarized in Table 3. Depending on the source of optical signals, MIP-based optical sensors can be divided into two types. The first are the MIP-affinity sensors that can be used to detect analytes with inherent optical properties (e.g. fluorescence and refractive index) (Ahmad et al., 2018). In these optial sensors, fluorescence detecting is the most popular method for the detection of FSHFs, making use of the fluorescence quenching caused by the electron/hole transfer between target molecules and fluorophores. Quantum dots (QDs) (Habimana et al., 2018; Wu et al., 2017a) and carbon dots (CDs) (Shirani et al., 2019; Xu and Lu, 2015) are the fluorophores commonly used. To prepare the fluorophores that are stable and suitable for the detection in food matrix, core-shell structures with silica coating (Yang et al., 2016) and MIP films (Ding et al., 2017) are built. MIP-based optical sensors are also designed based on specific optical properties of nanomaterials, such as surface enhanced Raman scattering strategy (SERS), resonance light scattering (RLS) and surface plasmon resonance (SPR) (Yang et al.,

Table 2
Performance of MIP-based electrochemical sensors for the detection of FSHFs.

Analyte		Food sample	Sensing system	Mode	LOD (M)	Ref.
Chemical hazards						
Natural toxins	Patulin	Apple juice	MIP-Au/CS-CDs/GCE	DPV	7.57×10^{-13}	Guo et al. (2017)
		Apple and grape juice	MIP-Pt NP/NGE/GCE	DPV	6.49×10^{-12}	Huang et al. (2019)
Pesticides	Hexazinone	Water	MIP/CPE	DPCSV	2.6×10^{-12}	Toro et al. (2015)
	Imidacloprid	Tomato, cabbage, chili, lettuce	BB doped MIP/Pt–In NPs/GCE	DPV	1.2×10^{-11}	Li et al. (2016a)
	Chlorpyrifos	n. d	MIP-B-TiO_2 NRs/FTO	Photocurrent response	2.2×10^{-14}	Sun et al. (2017)
	Methamidopho	Spiked cucumber, kidney bean	MIL@MIP/Fe_3O_4/rGO/CS	DPV	2.67×10^{-13}	Shi et al. (2017)
	Omethoate				2.05×10^{-14}	
	Carbofuran	Cabbage, celery, chili, onion, peppermint	MIP-CNTs-Fe_3O_4@Au/CPE	Amp	3.8×10^{-9}	Amatatongchai et al. (2018)
Fishery and veterinary drugs	Metronidazole	Tablet, fish meat	MIP/NPNi/GE	CV	2×10^{-14}	Li et al. (2015c)
	Diethylstilbestrol	Milk	Au NPs/MWCNTs-CS/sol-gel-MIP/GCE	DPV	9.055×10^{-13}	Bai et al. (2017)
	Olaquindox	Pork, fish	MIP/AuNPs/cMWCNTs/GCE	DPV	2.7×10^{-9}	Wang et al. (2017a)
	Salbutamol	Human urine, pork samples	MIP/Ag–N-RGO/GCE	DPV	7×10^{-9}	Li et al. (2017b)
	Sulfamethoxazole	Milk	MIP/Au	Amp	–	Turco et al. (2018)
	Chloramphenicol	n. d	MIP/PEDOT/LIG	EIS	6.2×10^{-8}	Cardoso et al. (2019)
	Sulfapyridine	Fish	MIP/α-$Ni(OH)_2$/NF	DPV	3.57×10^{-7}	Liu et al. (2019)
Environmental contaminants	Tributyltin	Sea water	MIP-Fe_3O_4 NPs/SPE	EIS	5.37×10^{-12}	Zamora-Gálvez et al. (2017)
Additives	Sunset yellow	Jelly, fruit drinks, chocolate, instant juice powder, ice cream, candy	MIP- MWCNTs/GCE	DPV	1.4×10^{-9}	Yin et al. (2018b)
	Melamine	Milk	MIP-MWCNTs/GCE	DPSV	5.6×10^{-13}	Xu et al. (2018)
Process and package contaminants	Bisphenol S	Mineral water, extraction solutions of plastic	MIP/GQDs/hNiNS/GQDs/GCE	CV	3×10^{-8}	Rao et al. (2018)
Biological hazards						
Fungal contaminations	Patulin	Apple juice	MIP-Au/CS-CDS/GCE.	DPV	7.57×10^{-13}	Guo et al. (2017)
Bacterial contaminations	N-acyl-homoserine-lactones	n. d	Fe_3O_4@SiO_2-MMIP/MGCE	DPV	8×10^{-10}	Jiang et al. (2016)

Differential pulse voltammetry (DPV), amperometry (Amp), differential pulse with cathodic stripping voltammetry (DPCSV), electrochemical impedance spectroscopy (EIS), cyclic voltammetry (CV), differential pulse stripping voltammetry (DPSV). Limit of detection (LOD). n. d = no data.

Table 3
Performance of MIP-based optical sensors for the detection of FSHFs.

Analyte		Food sample	Sensing system	Detection method	LOD	Ref.
Chemical hazards						
Natural toxins	Saxitoxin	Shellfish	MIP@ CdS/CdSe/ZnS QDs	Fluorescence	0.3 g/kg	Sun et al. (2018)
Pesticides	Cyphenothrin	River water	MIP@ ZnS:Mn QDs	Fluorescence	9×10^{-9} M	Ren and Chen (2015)
	Fenaminosulf	Lettuce, cabbage, tomato, banana	Neutral red doped MIP/Ag/ITO	Fluorescence	1.6×10^{-11} M	Li et al. (2015b)
	Chlorpyrifos	Drinking water	MIP/IrOx NPs/ITO SPEs	ECL	1×10^{-13} M	Capoferri et al. (2018)
	Cyfluthrin	Fish, sediment	MIP@ FeSe QDs	Fluorescence	2.3×10^{-9} M	Li et al. (2018c)
	Methanephosphonic acid	n. d	MIP@CCAs hydrogel particles	Colorimetry	1.0×10^{-6} M	Huang et al. (2018)
	Acetamiprid	Wastewater, apple	MIP@Si-CDs	Fluorescence	2×10^{-9} M	Shirani et al. (2019)
	Triazophos	Cabbage and apple	MIP film and THBu- CdSe/ZnS QDs	Fluorescence	9.89×10^{-10} M	She and Wang (2019)
Fishery and veterinary drugs	Tetracycline	Goat milk, pure milk	MIP@SiO_2–CdTe QDs	Fluorescence	1.4×10^{-7} M	Yang et al. (2016)
	Ciprofloxacin	n. d	MIPs-SPRi chip	SPR	–	Luo et al. (2016)
	Azithromycin	n. d	MIPs-SPRi chip	SPR	–	Luo et al. (2016)
	Enrofloxacin	Perch, catfish, Spanish mackerel	apta-MIP@UCNPs.	Luminescence	1.11×10^{-13} M	Liu et al. (2017b)
	Lincomycin	Chicken, duck, crucian, pork, crab, beef, mutton	CDs-apta-MIP/Au-GO NPs/GCE	ECL	1.6×10^{-13} M	Li et al. (2017c)
	17β-estradiol	Milk, human urine	MIP/Nylon membrane	Colorimetry	9.18×10^{-10} M	Xiao et al. (2017)
	Malachite green	Water, fish	MIP@ CdTe QDs	Fluorescence	5.9×10^{-8} M	Wu et al. (2017b)
	Clenbuterol	Pork, pig liver and pig kidney	MIP/UCNPs/rGO/GCE	ECL	6.3×10^{-9} M	Jin et al. (2018)
Environmental contaminants	Polycyclic aromatic hydrocarbons	Commercial milk	MIP@ Fe_3O_4/$LaVO_4$:Eu^{3+}	Luminescence	3.64 ng/mL	Li and Wang (2013)
Additives	Melamine	Raw milk, milk powder	MIP@CdTe QDs	Fluorescence	3.8×10^{-8} M	Xu and Lu (2015)
Process and package contaminants	Acrylamide	Potato chips, fried bread stick, rice crust, bread	MIP@Mn–ZnS QDs/rGO	Fluorescence	1.7×10^{-7} M	Liu et al. (2018)
	Bisphenol A	Lake water, tap water, pure milk	MIP@SiO_2@Ag NPs	SERS	1.46×10^{-11} M	Yin et al. (2018a)
Biological hazards						
Fungal contaminations	Sterigmatocystin	Corn, rice, and millet	MIP@CDs	Fluorescence	5.86×10^{-8} M	Xu et al. (2016)
	Patulin	Environmental water, apple juice	MIP-capped Ag NPs@ZnMOF	Fluorescence	6×10^{-8} M	Bagheri et al. (2018)
Viral contaminations	Hepatitis A virus	Human serum	MIP@SiO_2 NPs	RLS	8.6×10^{-12} M	Yang et al. (2017)
Bacterial contaminations	*Enterococcus faecalis*	Sea water	E. faecalis-imprinted NPs- SPR chip	SPR	6.8×10^{-8} M	Habimana et al. (2018)

Electrochemiluminescence (ECL), surface enhanced Raman scattering strategy (SERS), resonance light scattering (RLS), surface plasmon resonance (SPR). Limit of detection (LOD). n. d = no data.

2017; Yao et al., 2016; Yin et al., 2018a). The second are optoelectronic sensors. It is noteworthy that there have been research combining optoelectronic sensor with smartphone detection for potential rapid test of FHSFs (Capoferri et al., 2018).

Apart from electrochemical and optical sensors, other MIP-based sensors have also been used in FSHF detection. These include biomimetic enzyme-linked immunosorbent assay (ELISA) (Tang et al., 2017) and mass-sensitive sensors, such as QCM (Lin et al., 2018; Yang and Park, 2016). Though some FSHFs, such as protein, virus and bacteria, are large-molecule-targets with relatively large mass, owing to the disturbance of the food matrix, the existing mass-sensitive sensors are not significantly advantageous in practical detection of FSHFs.

4. Applications of MIP-based sensors in FSHF detection

Though the detection of most FSHFs can be realized, they may not fully meet the requirement of modern food industry. As a special commodity with limited profit and shelf life, food raises higher demand of reduced testing cost and time of FSHF detection. In addition, with generally low technical level of employees, easy-operating methods are necessary. However, due to the low content of FSHFs and complexity of food sample matrix, the FSHF detection requires sophisticated sample preparation and instruments, along with high operating technique and cost. Meanwhile, storage and transportation of food samples and the detection of multiple FSHFs in different laboratories will also delay distribution to consumers, which debase the quality of food (Dincer et al., 2019). Therefore, detection performed on-site by low-cost, easy and rapid testing methods with high sensitivity and selectivity is urgently needed for monitoring FSHFs in practical food production.

Recent researches have shown that MIP-based sensors have great potential in industrial application for FSHF detection, since they successfully combine the advantages of MIP receptors and various sensing platforms. According to the principle of their signal transductions, MIP-based sensors can be classified into MIP-based electrochemical, optical and other sensors. Some of the applications of different MIP-based sensors in FSHF detection in the past five years are discussed below.

4.1. MIP-based electrochemical sensors

MIP-based electrochemical sensors have been under active investigation in recent years (Table 2), offering potential for both qualitative and quantitative analysis.

A great amount of MIP-based electrochemical sensors has been designed for the detection of various chemical hazards. Pesticides, as well as fishery and veterinary drugs, are the most important targets. For the detection of chlorpyrifos, an organophosphorus pesticide for insect control, an MIP-based photoelectrochemical sensor was designed (Sun et al., 2017). Titanium dioxide nanorods (TiO_2 NRs) were grown directly on fluorine-doped tin oxide (FTO) by hydrothermal method, followed with growth of branches to form branched titanium dioxide nanorods (B–TiO_2 NRs). The MIP film was then electro-polymerized on the surface of B–TiO_2 NRs, using chlorpyrifo and p-aminothiophenol (PATP) as template molecule and functional monomer, respectively. After the removal of templates, the cavities specific to chlorpyrifo were formed (Fig. 4A). Combining the high photoelectric activity of B–TiO_2 NRs under UV irradiation and the recognition of MIPs, the combination between chlorpyrifo and the cavities in MIPs could hinder the harvesting of light and electron transfer with increasing chlorpyrifo concentration, making the photocurrent response inversely proportional to CPF concentration. B–TiO_2 NRs have improved sensitivity and selectivity of detection with a low detection limit of 7.4 pg/mL. Ultrasensitive detection of diethylstilbestrol was also realized by an MIP-based electrochemical sensor (Bai et al., 2017). To amplify the signal of the sensor, Au nanoparticles (Au NPs) and MWCNTs-chitosan composite (MWCNTs-CS) was used for layer-by-layer modification on bare GCE (Fig. 4B). During the following sol-gel imprinting, 3-aminopropyltriethoxysilane (APTES) was chosen as functional monomer because of its amino group that interacts with templates through hydrogen bonding. Tetraethoxysliane functions as a cross-linker to form a polymeric siloxane network through Si–O bond via hydrolysis. The obtained sensor not only showed good selectivity and long-term stability, but also realized the detection in milk samples. Recently, a novel nanomaterial, $Ni(OH)_2$ nanoarrays electrode was applied in MIP-based electrochemical sensors as sensing platform for the detection of sulfapyridine (Liu et al., 2019). The modified electrode was prepared in situ on nickel foam by hydrothermal methods. Next, the MIPs were directly imprinted on the surface of nanoarrays by the self-assembly of monomers (Fig. 4C). Instead of modifying the surface of electrode with pre-prepared structural materials, this strategy built complex stereochemical structure by handy electrode treatment. Compared with other methods, this strategy simplified the procedure of sensor development with just two steps, the preparation of electrode and molecularly imprinting, showing better feasibility in mass production. Similar strategies have also been developed for the detection of metronidazole (Li et al., 2015a, 2015c; Song et al., 2016).

In addition, the industrialization of food production calls for the monitoring of food additives and processing and packaging contaminants. Different from the above-mentioned MIP-based electrochemical sensor modified with MWCNTs, Xu et al. provided another strategy to assemble MWCNTs with MIPs (Xu et al., 2018). MIP-MWCNTs units with “necklace-like” nanostructures were generated by incorporating MWCNTs in the co-assembly process of a photo-cross-linkable copolymer poly (acrylic acid-*co*-(7-(4-vinylbenzyloxy)-4-methyl coumarin)-co-ethylhexyl acrylate) (poly (AA-*co*-VMc-*co*-EHA)) (PAVE) and templates, in which there were intermolecular charge and electronic energy transfer between MIP “beads” and MWCNT “axis”. Then the MIP-MWCNTs units were cast on bare electrode (Fig. 4D). Using $[Fe(CN)_6]^{3-/4-}$ as the electrochemical probe, the rebinding of melamine in MIPs obstructed the electron transfer across the electrode surface. With the significant linear relationship between the variation of decreased oxidation peak current and logarithm of melamine concentration, this sensor realized the quantification of melamine (1.0×10^{-12}-1.0×10^{-6} M). Making use of the high affinity and specificity of DNA to targets, MIPs was combined with ds-DNA for dual recognition of Sudan II in MIP-based electrochemical sensors (Rezaei et al., 2016). Prior to the polymerization, Sudan II was let interact with ds-DNA. By the electro-polymerization of functional monomers, *o*-phenylenediamine, ds-DNA and Au NPs were entrapped into the MIP film and realized dual recognition. In this complex MIP film, polymer not only formed a stable 3D structure but also provided phenyl and –NH groups to interact with Sudan II via π-π interactions and hydrogen bonding. Due to the cooperation between ds-DNA and MIPs, this sensor showed better selectivity to Sudan II compared with conventional imprinted sensors. Ensafi et al. developed a similar method for the detection of bisphenol A (Ensafi et al., 2018). Besides, the application of multiple nanomaterials is also a strategy to build MIP-based electrochemical sensors for bisphenol S detection (Rao et al., 2018). Hollow nickel nanospheres were firstly modified on GCE by dealloying Cu from the Ni–Cu alloy, transforming small alloy blocks into hollow nickel nanospheres. The graphene quantum dots were then coated on the modified GCE. After the electropolymerization of pyrrole in the presence of templates, this sensor realized sensitive detection according to the specific hydrogen bonding and π-π stacking interactions between MIPs and bisphenol S (Fig. 4E). With the development of micromachining technology, microfluidic chip has also been used in the preparation of MIP-based electrochemical sensors to establish a dual identification system for carbofuran detection (Li et al., 2018b). Instead of integrating the recognition units in the same region, MIPs and aptamer were respectively modified on two functional areas, connected by a channel (Fig. 4F). When the test samples were transported in microfluidic chip by a micro-pump, the carbofuran was firstly gathered in MIPs of the first functional area, then the captured carbofuran targets

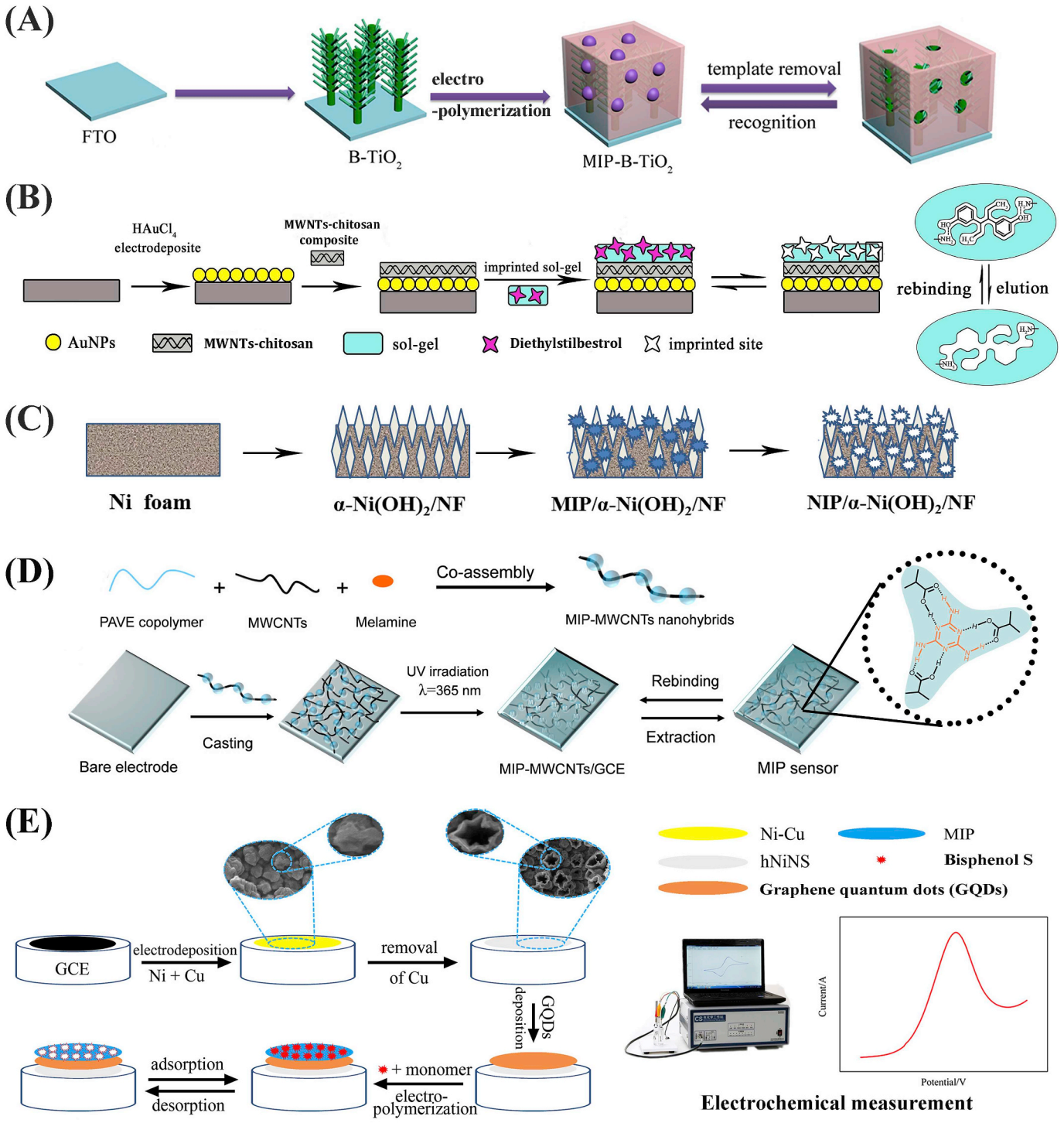

(caption on next page)

Fig. 4. (A) Schematic for the fabrication of chlorpyrifos-imprinted electrochemical sensor. Reprint from Sun et al. (2017) with permission from Elsevier. (B) Schematic for the fabrication of diethylstilbestrol-imprinted electrochemical sensor. Reprint from Bai et al. (2017) with permission from Elsevier. (C) Schematic for the fabrication of sulfapyridine-imprinted electrochemical sensor. Reprint from Liu et al. (2019) with permission from Elsevier. (D) Schematic for the fabrication of melamine-imprinted electrochemical sensor. Reprint from Xu et al. (2018) with permission from American Chemical Society. (E) Schematic for the fabrication of bisphenol S-imprinted electrochemical sensor. Reprint from Rao et al. (2018) with permission from Elsevier. (F) Schematic for the fabrication of carbofuran-imprinted electrochemical sensor. Reprint from Li et al. (2018b) with permission from Springer Nature.

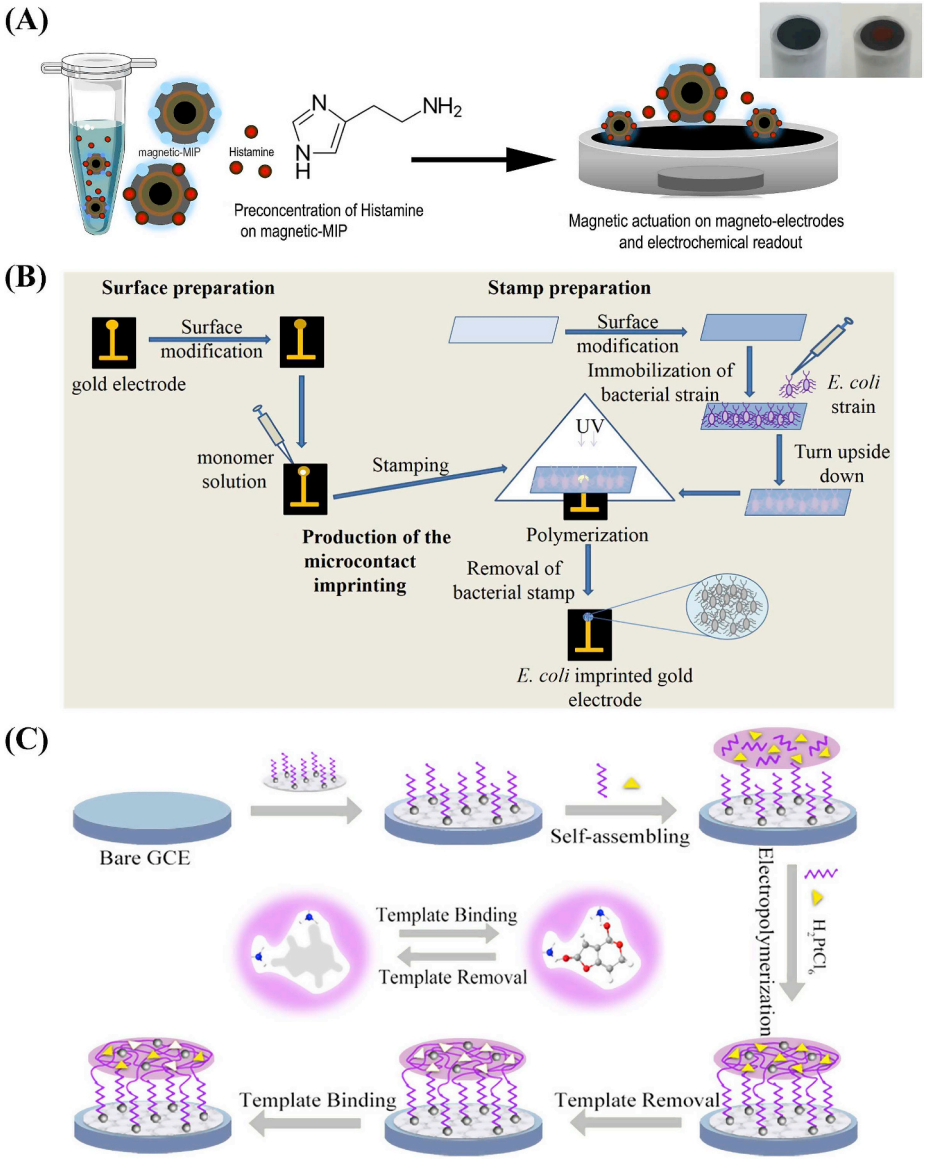

Fig. 5. (A) Schematic for the fabrication of scombrotoxin-imprinted electrochemical sensor. Reprint from Hassan et al. (2019) with permission from Elsevier. (B) Schematic for the fabrication of *Escherichia coli*-imprinted electrochemical sensor. Reprint from Idil et al. (2017) with permission from Elsevier. (C) Schematic for the fabrication of patulin-imprinted electrochemical sensor. Reprint from Huang et al. (2019) with permission from American Chemical Society.

were eluted off and transported to the next functional area with aptamer for electrochemical detection. Microfluidic chips make the modularization of MIP-based electrochemical sensors possible, which facilitates their commercial production.

Apart from these exogenous chemical hazards, MIP-based electrochemical sensors are also designed for the detection of endogenous natural toxins in food. Accumulation of biogenic amines in food is mainly caused by the presence of bacteria with decarboxylation activity. Therefore, histamine content has recently become an important index for monitoring food safety, quality and freshness (Shalaby, 1996). Recently, making used of the separation ability of permanent magnet, detachable sensor based on core-shell structural magnetic MIPs has been reported (Hassan et al., 2019). Modified with tetraethyl orthosilicate and 3-methacryloxypropyltrimethyloxysilane, Fe_3O_4 nanoparticles was prepared as magnetic core. Computer simulation was applied for the design of MIPs, and MIP shell was coated on magnetic core using 2-vinyl pyridine and EGDMA as monomer and cross-linker, respectively. Instead of assembling receptors on the electrode permanently, this sensor firstly pre-concentrated targets by mixing magnetic MIPs with samples and then integrated magnetic MIPs into magneto-actuated electrodes for direct electrochemical detection of histamine (Fig. 5A). With a low detection limit (1.6×10^{-6} mg/L), this simple and rapid method provided a novel strategy to apply MIPs and magneto-actuated device in food analysis.

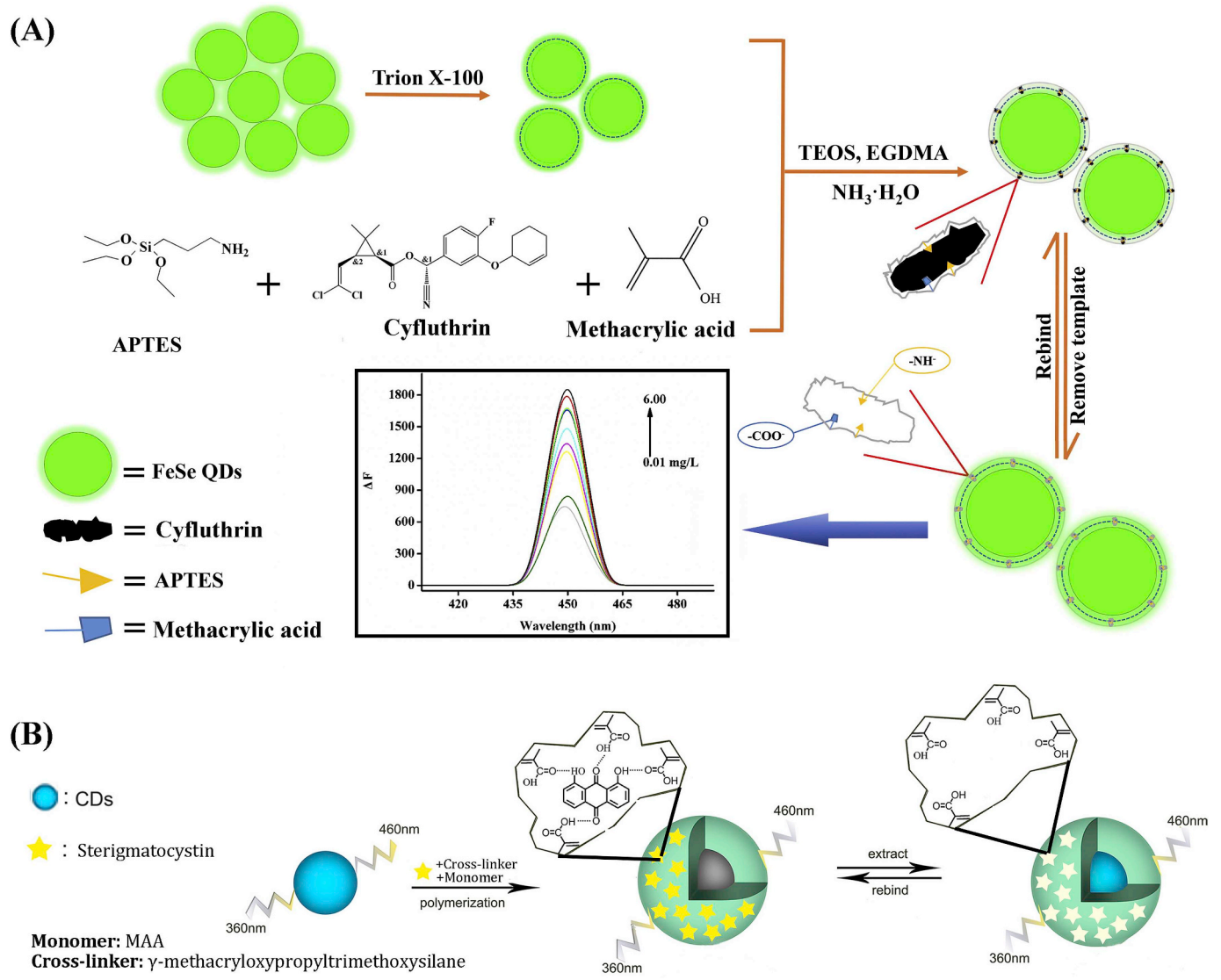

Fig. 6. (A) Schematic for the fabrication of MIP-FeSe-QDs. Inset: fluorescence spectra of MIP-QDs with increased cyfluthrin concentration. Reprint from Li et al. (2018c) with permission from Elsevier. (B) Schematic for the fabrication of MIP-CDs. Reprint from Xu et al. (2016) with permission from Elsevier.

A number of MIP-based electrochemical sensors have been reported for the detection of biological hazards. For the detection of *Escherichia coli*, Idil et al. developed an MIP-based capacitive sensor (Idil et al., 2017). Because the templates, *Escherichia coli*, are whole cells with large volume and complex structure, microcontact imprinting technology was applied for surface imprinting (Fig. 5B). *Escherichia coli* cells were firstly immobilized on the surface of glass slide. Next, the templates were brought into contact with the monomer mixture covering the capacitive gold electrode surface by turning the modified glass slide upside down. After UV photo-polymerization and removal of bacterial stamp, this sensor realized real-time *Escherichia coli* detection within the range of 1.0×10^2–1.0×10^7 CFU/mL. There have been only a few reports focused on whole cell imprinting, so this study provides a great model for the detection of pathogenic bacteria and spoilage bacteria. Fungal contaminants are also major biological hazards, while studies on the MIP-based electrochemical sensors for fungal contaminants detection are limited. Recently, thionine was applied as both functional monomer and signal indicator to form novel electrochemical sensors for the detection of patulin (Huang et al., 2019). With two amino groups, thionine can not only form poly (thionine) film, but also drives patulin targets into the MIP specific cavities through hydrogen bond. By electropolymerization, molecularly imprinted poly (thionine) was synthesized on the Pt nanoparticles (Pt NPs)-nitrogendoped graphene modified GCE (Fig. 5C). Though functional monomer has good electron transfer ability, the combination of patulin and MIPs could decrease the electric conductivity of MIP film, decreasing the reduction peak current. Therefore, this sensor displayed an excellent performance for patulin detection over the range of 0.002–2 ng/mL with a detection limit of 0.001 ng/mL and successfully detected patulin in real apple and grape juice samples.

4.2. MIP-based optical sensors

The major optical techniques applied in MIP-based optical sensors include fluorescence monitoring, electrochemiluminescence (ECL), surface enhanced Raman scattering strategy (SERS), resonance light scattering (RLS) and surface plasmon resonance (SPR) (Table 3).

Fluorescence monitoring has been the most popular technique because of the simplicity of the preparation and the low testing limits attainable (Ahmad et al., 2019). Owing to their unique optical properties of narrow emission and resistance to fluorescence quenching, QDs have great potential as fluorescent sensors, probes, and tags (Ren and Chen, 2015). For the detection of cyfluthrin, an important broad-spectrum pesticide, molecularly imprinted silica film was coated on

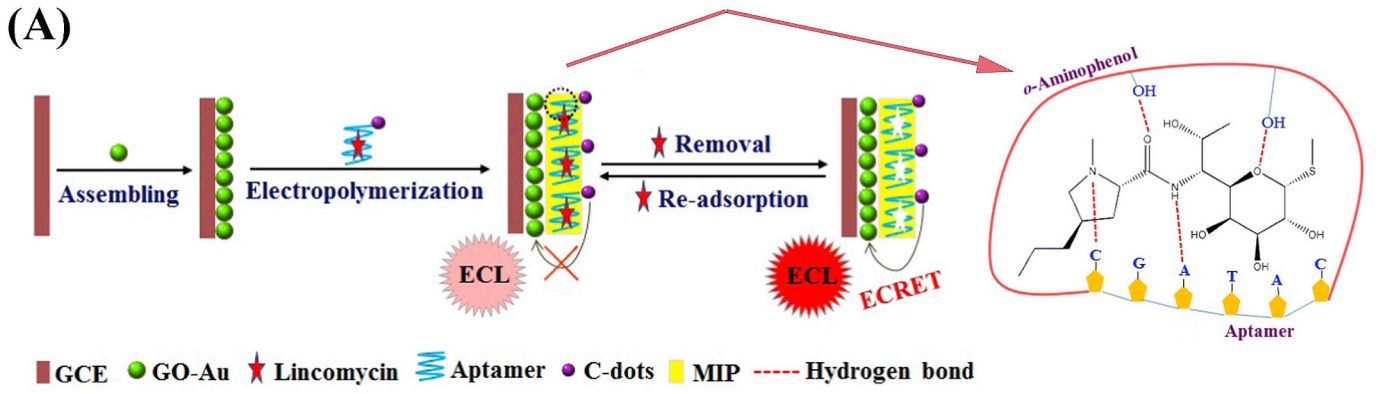

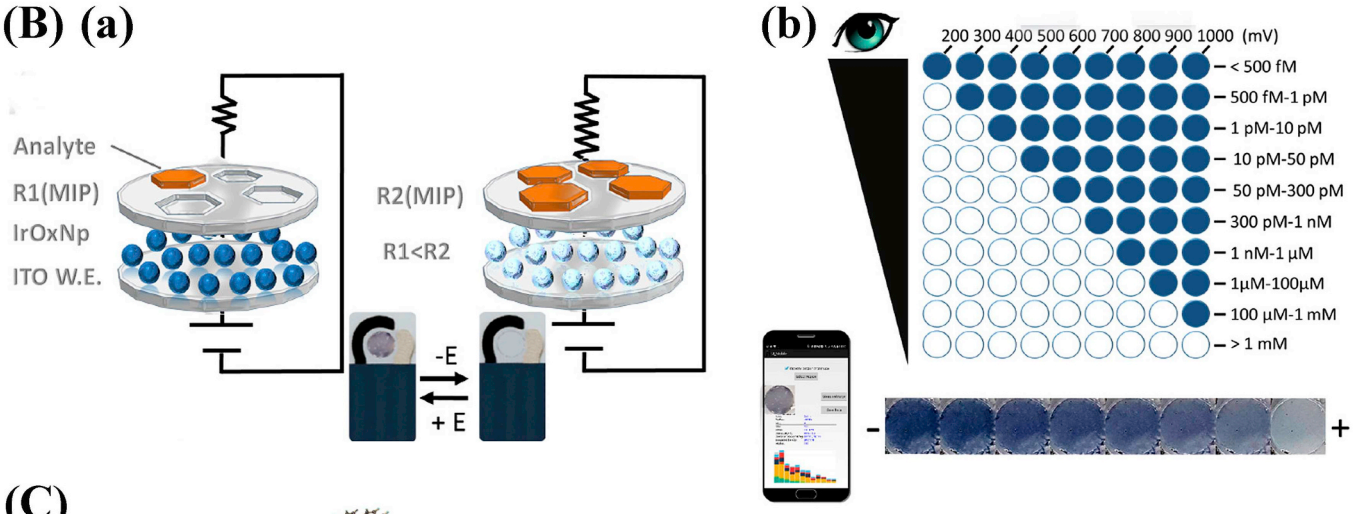

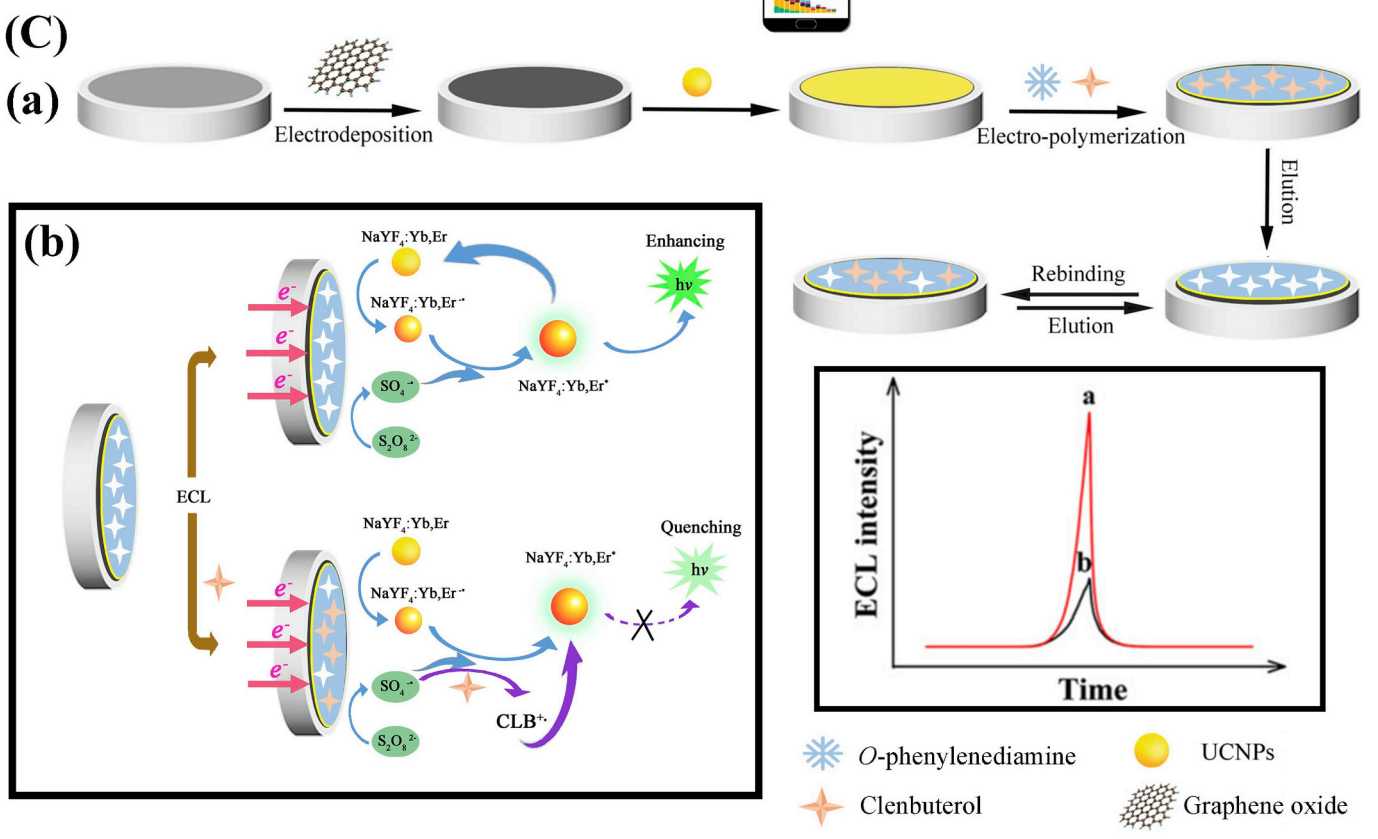

(caption on next page)

Fig. 7. (A) Schematic for the fabrication of lincomycin-imprinted optical sensor. Reprint from Li et al. (2017c) with permission from Elsevier. (B) (a) Schematic for the MIP/IrOx NPs-ITO SPEs structure, visual IrOx NPs color change (from blue-black to transparent), and working principle of the proposed sensor with different analyte amounts; (b) Visual detection after 10 s of the application of different oxidation potentials, as well as smartphonebased detection of concentration ranges detected based on the number of colored electrodes and change of IrOx NPs color intensity at a fixed time and potential vs increasing amounts of the analyte. Reprint from Capoferri et al. (2018) with permission from American Chemical Society. (C) (a) Schematic for the fabrication of clenbuterol-imprinted optical sensor; (b) ECL mechanism and the quenching mechanism of clenbuterol towards MIP-based electrochemiluminescence sensor. Reprint from Jin et al. (2018) with permission from Elsevier. (For interpretation of the references to color in this figure legend, the reader is referred to the Web version of this article.)

FeSe QDs by reverse micro-emulsion polymerization (Li et al., 2018c) (Fig. 6A). During the detection, ionic interaction and hydrogen bond could be formed between cyfluthrin and MIPs for specific recognition. Meanwhile, the charge transfer from the FeSe-QDs to cyfluthrin could be blocked, resulting in the fluorescence quenching of the MIP-FeSe-QDs. This method realized monitoring in fish samples with a detection limit of 1.0 μg/kg. Besides, CdTe QDs (Yang et al., 2016) and Mn(II)-doped ZnS QDs (Liu et al., 2018) have also been combined with MIPs for the detection of FSHFs. However, these conventional semiconducting QDs have some drawbacks, such as biological toxicity and environmental pollution. Recently, CDs have attracted attention because of their stable photoluminescence, green synthesis, biocompatibility and other excellent properties (Shirani et al., 2019). For instance, high blue luminescent CDs were embedded into MIPs by non-hydrolytic sol-gel process for the detection of sterigmatocystin, using 1,8-dihydroxyanthraquinone as an alternative template (Xu et al., 2016) (Fig. 6B). The sterigmatocystin in samples could be drawn into the cavities by hydrogen binding with MIPs, and the bound sterigmatocystin would accept the electrons from CDs, quenching fluorescence.

ECL is a method to translate electrochemical signals to optical signals, and the combination of both electro and optical properties can improve sensing capabilities (Ahmad et al., 2019). A platform based on electrogenerated chemiluminescence energy transfer was reported for the detection of lincomycin (Li et al., 2017c). To improve selectivity and sensitivity of the whole sensor, lincomycin-CD-tagged aptamer complexes were pre-assembled as alternative templates for imprinting (Fig. 7A). After elution, lincomycin molecules were removed, while CD-tagged aptamers remained embedded in the MIP layer. At a specific voltage, CDs were stimulated to product ECL signal. Drawn by dual recognition, lincomycin could enter the identification sites on the MIPs and combine with aptamers, leading to the structural change which attenuated the transfer of energy from modified electrode to CDs. Therefore, the intensity of the electrogenerated chemiluminescence response was inversely proportional to lincomycin concentration. ECL also shows great potential to combine with smartphone-based detection. Based on Iridium oxide (IrOX), an electrochromic material with optical properties to generate large spectral shifts among its multiple oxidation states, Capoferri et al. took advantage of MIPs, IrOX NPs and transparent ITO SPE to build an MIP-based electrochromic sensor for the detection of chlorpyrifos (Capoferri et al., 2018). The targets in MIP cavities decreased the conductivity of molecularly imprinted polypurrole and simultaneously decreased the oxidation current of IrOX NPs, lightning the color of the whole sensor. Thus, chlorpyrifos concentration can be evaluated roughly with both naked eye and smartphone (Fig. 7B). Although this method does not accurately quantify the concentration of pesticide residues, its dependence on on color variation makes it useful for in situ screening analysis. As a new generation of ECL material, upconversion nanoparticles (UCNPs) was also applied for the detection of clenbuterol, a forbidden animal growth promoter (Jin et al., 2018). Reduced graphene oxide (rGO), UCNPs and MIPs were fabricated on the surface of GCE as signal amplifying agent, luminophor and receptor, respectively (Fig. 7C). The recombination of target clenbuterol with cavities in MIPs could block electron transport channels between UCNPs and coreactant $K_2S_2O_8$, thus the ECL intensity decreased along with increasing clenbuterol concentration, displaying a linear relation between ECL intensity and clenbuterol concentrations ranging from 10 nM to 100 μM.

MIP-based optical sensors based on SPR, SERS and RLS have few applications in the detection of FSHFs. More than one MIP spots can be synthesized on the surface of a modified SPR gold chip by multiple UV-initiated polymerizations, controlling the area of MIPs with the help of a mask to cover other parts of the chip (Fig. 8A). Therefore, SPR sensors have achieved simultaneous multiple detection of fishery and veterinary drugs (Luo et al., 2016). However, due to its heavy dependence on expensive materials and equipment, as well as complex pretreatment process, this sensor cannot achieve on-site monitoring of FSHFs. Based on the unique optical properties of nanoparticles, a SERS-MIP and RLS sensor has been developed for the detection of FSHFs. Making use of plasmon resonance between silver particles and shell layer, Yin et al. designed a reapberry-type SiO_2@Ag NPs to enhance plasmonic (Yin et al., 2018a). Followed by non-covalent imprinting, bisphenol A-imprinted polymer shell was obtained at the outer edge (Fig. 8B–D). This sensor was applied in the detection of water and milk samples, with the recovery of 89.98–111.31%. An MIP-based RSL sensor was employed for the detection of Hepatitis A Virus (HAV) (Yang et al., 2017). Because of the easily denatured protein coat of HAV, the core-shell structure was built on SiO_2 NPs taking advantage of the mild self-polymerization of virus-imprinted polydopamine (Fig. 8E and F). The MIP film could effectively capture HAV on the surface of MIP- SiO_2 NPs and cause changes in RSL intensity, which could be measured by a simple fluorescence spectrophotometer. Therefore, this research provided an interesting strategy to expand the application of MIP-based optical sensors to the determination of virus.

4.3. Mass-sensitive MIP-based sensors

There are few studies on the application of mass-sensitive MIP-based sensors in FHSF detection. With the steady and accurate quartz crystal resonators, QCM can monitor the change of mass by frequency measurements and has attracted some attention on the detection of large biotemplates, such as bacteria and virus (Jia et al., 2018). For the determination of *Escherichia coli*, pre-mixed imprint materials containing Epon1002F were firstly spin coated on the QCM (Poller et al., 2017). The obtained QCM was further spin coated with stamp materials inked with *Escherichia coli.* The imprint stamp was prepared with glucose, as a blocker, to prevent the covalent binding between MIPs and template bacteria, which contributed to the removal of templates. Using commercially available material as the imprint material, this sensor displayed commercialization potential. However, more research is needed before it can be applied in the detection in real food samples. In addition, although MIP-based sensors with microcantilevers have been used for the detection of fishery and veterinary drugs in air, due to difficulties in overcoming liquid damping in food matrix, they have not been applied to analyze actual samples (Okan et al., 2017; Okan and Duman, 2018).

5. Summary and conclusions

In this review, research advances of MIP-based sensors in FSHF detection in the past 5 years have been systematically summarized according to sensing mechanisms, including electrochemistry, optics and mass-sensitivity. Among various MIP-based sensors, electrochemical and optical sensors have been widely used. They are mainly

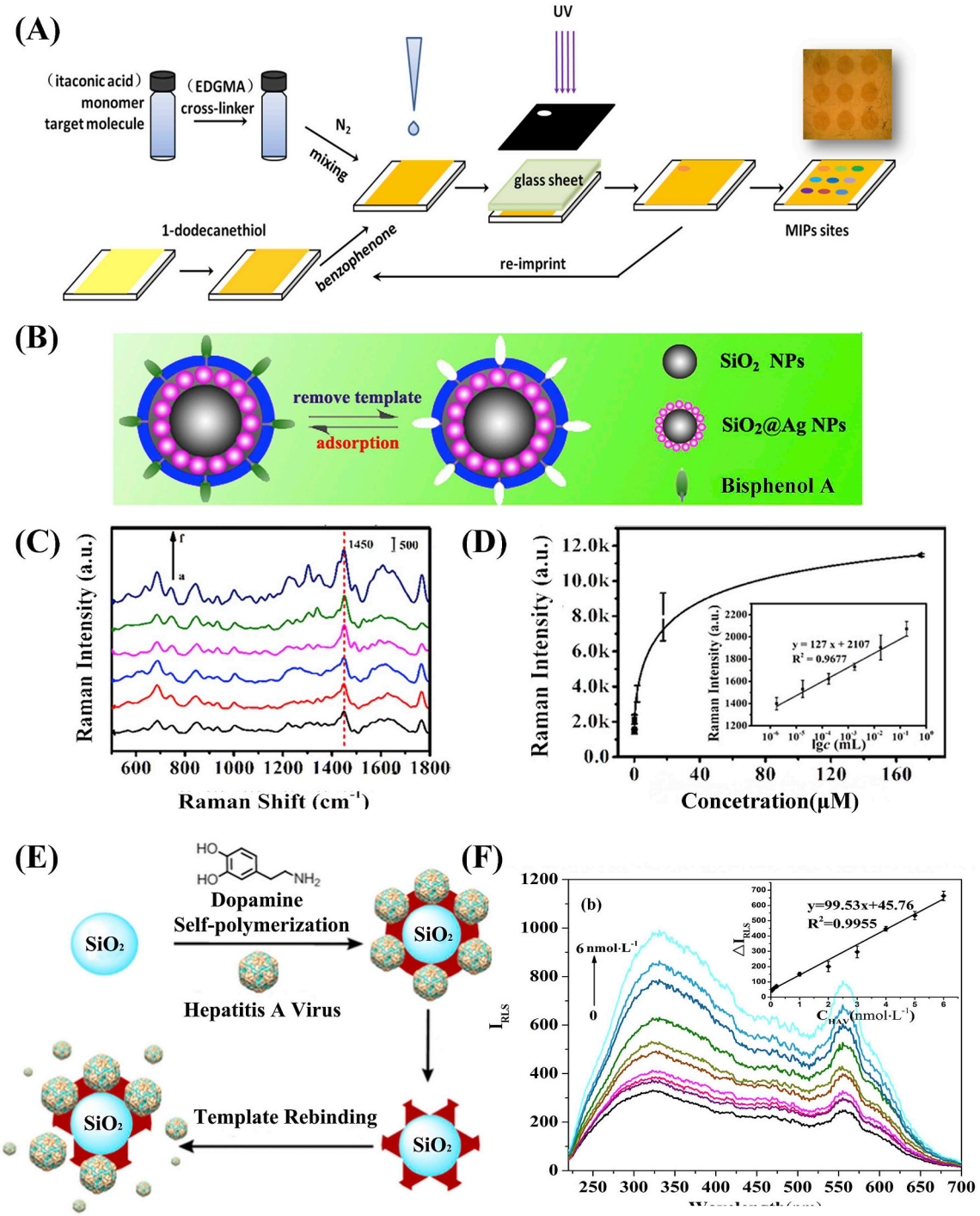

Fig. 8. (A) Schematic for the fabrication of ciprofloxacin-imprinted SPR sensor. Reprint from Luo et al. (2016) with permission from Elsevier. (B) Schematic for the SERS- (bisphenol A-imprinted polymer) sensor; (C) SERS spectra of MIP-ir-SiO2@Ag NPs incubated with different concentrations of bisphenol A solution. a–f: (1.75×10^{-11} to 1.75×10^{-6} M); (D) Plots of intensity versus bisphenol A concentrations corresponding to (C) at 1450 cm^{-1} based on MIP-ir-SiO2@Ag NPs. Inset: the liner relationship between the SERS intensity and the concentration of bisphenol A within the range from 1.75×10^{-11} to 1.75×10^{-6} M. Reprint from Yin et al. (2018a) with permission from Elsevier. (E) Schematic for the fabrication of Hepatitis A Virus-imprinted RLS sensor; (F) Effect of the indicated concentration of Hepatitis A Virus (0, 0.04, 0.1, 0.2, 1.0, 2.0, 3.0, 4.0, 5.0, 6.0 nM) on RLS spectra of Hepatitis A Virus -imprinted SiO2@PDA NPs. Inset: the liner relationship between the RLS intensity and the concentration of Hepatitis A Virus within the range from 0.04 to 6.0 nM (Condition: nanospheres dosage: 0.90 μg/mL, pH: 6.2, temperature: 25 °C). Reprint from Yang et al. (2017) with permission from Elsevier.

fabricated for the detection of pesticides and fishery and veterinary drugs. With the application of new materials with improved properties, novel modifications of surface and microfabrication techniques in advanced MIP-based sensors, the FSHF detection targets have been expanded to range from small molecules to huge molecules, such as mycotoxins, virus and bacteria. Higher sensitivity and selectivity are simultaneously being achieved. MIP-based sensors can offer multiple advantages, such as portability, rapid response, simplicity and low-cost; therefore, they have enormous potential as portable devices for use by non-specialists for the detection of FSHFs, especially pesticides and

fishery and veterinary drugs. In the next few years, MIP-based sensors are predicted to gain more attention and grow at an even faster pace before releasing their full potential for the detection of FSHFs.

6. Future perspectives

Combining exquisite sensitivity and specificity of biological receptors with the convenience and processability of polymers (Uzun and Turner, 2016), MIP-based sensors have increasing potential for FSHF analysis. However, non-selective binding sites in MIPs and non-specific adsorption to the surface of MIP receptors may lead to non-specific binding, undesired adsorption and incomplete removal of templates. Considering the complex matrix compounds of food samples and target molecules with low-abundance, current MIP receptors' lack of ultra-selectivity and affinity is further recognized. In practical FSHF detection, especially on-site, rapid detection, sensors are only helpful if accurate quantitation of an analyte is accomplished within a reasonable timeframe (Wu et al., 2018). The response times of existing MIP-based sensors in practical food inspection are still less optimal. In addition, commercialization of MIP-based sensors is hindered by the complexity in fabricating MIP receptors on the sensor surface and limited reusability. Collectively, MIP-based sensors are still in their infancy and several outstanding issues remain to be addressed.

Many opportunities exist to improve the performance of MIP-based sensors for the detection of FSHFs. (i) Theoretical calculation may be used as a supplement to experience and experiment for screening functional monomers and optimizing polymerisation strategies. (ii) The exploitation of advanced materials with superior properties as functional monomers and cross-linkers of MIPs may improve selective chemical recognition of existing and potential FSHF detection targets. (iii) The design of multiple recognition combinations including MIPs and the application of dummy templates may be explored. (iv) Novel MIPs, such as imprinted hydrogel, may be developed for the detection of macromolecular FSHFs, including the whole pathogenic bacteria cells, foodborne virus and food allergen. (v) MIPs may join forces with other advanced technologies, such as nanotechnology, artificial intelligence and lab-on-a-chip technology. Development in these field may not only address outstanding issues of current MIPs, but also significantly expand their capability.

Declaration of interests

The authors declare that they have no known competing financial interests or personal relationships that could have appeared to influence the work reported in this paper.

The authors declare the following financial interests/personal relationships which may be considered as potential competing interests:

CRediT authorship contribution statement

Yunrui Cao: Conceptualization, Writing - original draft, Visualization. **Tingyu Feng:** Writing - review & editing. **Jie Xu:** Writing - review & editing, Supervision, Project administration. **Changhu Xue:** Supervision, Funding acquisition.

Acknowledgements

This work was supported by a grant from Agricultural Industry System of Ministry of Agriculture of the People's Republic of China (No. CARS-49 201702020).

References

Abdel-Ghany, M.F., Hussein, L.A., El Azab, N.F., 2017. Talanta 164, 518–528.
Ahmad, O.S., Bedwell, T.S., Esen, C., Garcia-Cruz, A., Piletsky, S.A., 2018. Trends Biotechnol. 1–16.
Ahmad, O.S., Bedwell, T.S., Esen, C., Garcia-cruz, A., Piletsky, A., Le, L., 2019. Trends Biotechnol. 37, 294–309.
Altintas, Z., Gittens, M., Guerreiro, A., Thompson, K.A., Walker, J., Piletsky, S., Tothill, I.E., 2015. Anal. Chem. 87, 6801–6807.
Amatatongchai, M., Sroysee, W., Jarujamrus, P., Nacapricha, D., Lieberzeit, P.A., 2018. Talanta 179, 700–709.
Ashley, J., Shahbazi, M.A., Kant, K., Chidambara, V.A., Wolff, A., Bang, D.D., Sun, Y., 2017. Biosens. Bioelectron. 91, 606–615.
Bagheri, N., Khataee, A., Habibi, B., Hassanzadeh, J., 2018. Talanta 179, 710–718.
Bai, J., Zhang, X., Peng, Y., Hong, X., Liu, Y., Jiang, S., Ning, B., Gao, Z., 2017. Sens. Actuators, B 238, 420–426.
Barreda-García, S., Miranda-Castro, R., De-los-Santos-Álvarez, N., Lobo-Castañón, M.J., 2018. Sens. Actuators, B 268, 438–445.
Basozabal, I., Guerreiro, A., Gomez-Caballero, A., Goicolea, M.A., Barrio, R.J., 2014. Biosens. Bioelectron. 58, 138–144.
Beloglazova, N.V., Lenain, P., De Rycke, E., Goryacheva, I.Y., Knopp, D., De Saeger, S., 2018. Talanta 190, 219–225.
Betlem, K., Mahmood, I., Seixas, R.D., Sadiki, I., Raimbault, R.L.D., Foster, C.W., Crapnell, R.D., 2019. Chem. Eng. J. 359, 505–517.
Cai, Y., He, X., Lei, P., Liu, J., Bin, Z., Jie, B., Zhang, T., 2019. Food Chem. 280, 103–109.
Cao, X., Zhao, F., Jiang, Z., Hong, S., Zhang, C., She, Y., Jin, F., Jin, M., Wang, J., 2018. Food Anal. Methods 11, 1435–1443.
Capoferri, D., Del Carlo, M., Ntshongontshi, N., Iwuoha, E.I., Sergi, M., Di Ottavio, F., Compagnone, D., 2017. Talanta 174, 599–604.
Capoferri, D., Álvarez-Diduk, R., Del Carlo, M., Compagnone, D., Merkoçi, A., 2018. Anal. Chem. 90, 5850–5856.
Cardoso, A.R., Marques, A.C., Santos, L., Carvalho, A.F., Costa, F.M., Martins, R., Sales, M.G.F., Fortunato, E., 2019. Biosens. Bioelectron. 124, 167–175.
Chmangui, A., Ridha, M., Touil, S., Bermejo-barrera, P., 2019. Talanta 199, 65–71.
Chunta, S., Suedee, R., Lieberzeit, P.A., 2018. Anal. Bioanal. Chem. 410, 875–883.
Cieplak, M., Kutner, W., 2016. Trends Biotechnol. 34, 922–941.
Dadkhah, S., Ziaei, E., Mehdinia, A., Baradaran Kayyal, T., Jabbari, A., 2016. Microchim. Acta 183, 1933–1941.
Dechtrirat, D., Yingyuad, P., Prajongtat, P., Chuenchom, L., Sriprachuabwong, C., Tuantranont, A., Tang, I.M., 2018. Microchim. Acta 185, 261–269.
Dincer, C., Bruch, R., Costa-rama, E., Fernández-abedul, M.T., Merkoçi, A., Manz, A., Urban, G.A., Güder, F., 2019. Adv. Mater. 31, 1806739.
Ding, H., Jiao, H., Shi, X., Sun, A., Guo, X., Li, D., Chen, J., 2017. Sens. Actuators, B 246, 510–517.
Eersels, K., Lieberzeit, P., Wagner, P., 2016. ACS Sens. 1, 1171–1187.
El-Kosasy, A.M., Kamel, A.H., Hussin, L.A., Ayad, M.F., Fares, N.V., 2018. Food Chem. 250, 188–196.
Elshafey, R., Radi, A.E., 2018. J. Electroanal. Chem. 813, 171–177.
Ensafi, A.A., Amini, M., Rezaei, B., 2018. Microchim. Acta 185, 265–271.
Fan, L., Hao, Q., Kan, X., 2018. Sens. Actuators, B 256, 520–527.
Fang, G., Wang, H., Yang, Y., Liu, G., Wang, S., 2016. Sens. Actuators, B 237, 239–246.
Fang, G., Yang, Y., Zhu, H., Qi, Y., Liu, J., Liu, H., Wang, S., 2017. Sens. Actuators, B 251, 720–728.
Fang, M., Zhou, L., Zhang, H., Liu, L., Gong, Z., 2019. Food Chem. 274, 156–161.
Guo, W., Pi, F., Zhang, H., Sun, J., Zhang, Y., Sun, X., 2017. Biosens. Bioelectron. 98, 299–304.
Habimana, J.D.D., Ji, J., Pi, F., Karangwa, E., Sun, J., Guo, W., Cui, F., Shao, J., Ntakirutimana, C., Sun, X., 2018. Anal. Chim. Acta 1031, 134–144.
Hassan, A.H.A., Sappia, L., Lima, S., Ali, F.H.M., Moselhy, W.A., Taboada, P., Isabel, M., 2019. Talanta 194, 997–1004.
Hong, E., Lee, S.Y., Jeong, J.Y., Park, J.M., Kim, B.H., Kwon, K., Chun, H.S., 2017. J. Sci. Food Agric. 97, 3877–3896.
Huang, C., Cheng, Y., Gao, Z., Zhang, H., Wei, J., 2018. Sens. Actuators, B 273, 1705–1712.
Huang, Q., Zhao, Z., Nie, D., Jiang, K., Guo, W., Fan, K., Zhang, Z., Meng, J., Wu, Y., Han, Z., 2019. Anal. Chem. 91, 4116–4123.
Idil, N., Hedström, M., Denizli, A., Mattiasson, B., 2017. Biosens. Bioelectron. 87, 807–815.
Jia, M., Zhang, Z., Li, J., Ma, X., Chen, L., Yang, X., 2018. TrAC Trends Anal. Chem. (Reference Ed.) 106, 190–201.
Jia, B., He, X., Lei, P., Xiang, J., Ping, J., 2019. Anal. Chim. Acta 1063, 136–143.
Jiang, H., Jiang, D., Shao, J., Sun, X., 2016. Biosens. Bioelectron. 75, 411–419.
Jin, X., Fang, G., Pan, M., Yang, Y., Bai, X., Wang, S., 2018. Biosens. Bioelectron. 102, 357–364.
Karimian, N., Stortini, A.M., Moretto, L.M., Costantino, C., Bogialli, S., Ugo, P., 2018. ACS Sens. 3, 1291–1298.
Kaushal, S., Priyadarshi, N., Kumar, A., Soni, S., Deep, A., 2019. Sensor. Actuator. B Chem. 289, 207–215.
Li, H., Wang, L., 2013. ACS Appl. Mater. Interfaces 5, 10502–10509.
Li, Y., Liu, Y., Liu, J., Liu, J., Tang, H., Cao, C., Zhao, D., Ding, Y., 2015a. Sci. Rep. 5, 33–35.
Li, S., Yin, G., Zhang, Q., Li, C., Luo, J., Xu, Z., Qin, A., 2015b. Biosens. Bioelectron. 71, 342–347.
Li, Y., Liu, Y., Yang, Y., Yu, F., Liu, J., Song, H., Liu, J., Tang, H., Ye, B.C., Sun, Z., 2015c. ACS Appl. Mater. Interfaces 7, 15479–15480.
Li, S., Liu, C., Yin, G., Luo, J., Zhang, Z., Xie, Y., 2016a. Microchim. Acta 183, 3101–3109.
Li, S., Yin, G., Wu, X., Liu, C., Luo, J., 2016b. Electrochim. Acta 188, 294–300.
Li, H., Li, N., Jiang, J., Chen, D., Xu, Q., Li, H., He, J., Lu, J., 2017a. Sens. Actuators, B 246, 286–292.
Li, J., Xu, Z., Liu, M., Deng, P., Tang, S., Jiang, J., Feng, H., Qian, D., He, L., 2017b. Biosens. Bioelectron. 90, 210–216.

Li, S., Liu, C., Yin, G., Zhang, Q., Luo, J., Wu, N., 2017c. Biosens. Bioelectron. 91, 687–691.
Li, S., Li, J., Luo, J., Zhang, Q., Zhang, L., 2017d. RSC Adv. 7, 56359–56364.
Li, H., Wang, X., Wang, Z., Wang, Y., Dai, J., Gao, L., Wei, M., Yan, Y., Li, C., 2018a. Microchim. Acta 185, 193–202.
Li, S., Li, J., Luo, J., Xu, Z., Ma, X., 2018b. Microchim. Acta 185, 1–8.
Li, X., Jiao, H.F., Shi, X.Z., Sun, A., Wang, X., Chai, J., Li, D.X., Chen, J., 2018c. Biosens. Bioelectron. 99, 268–273.
Li, Lei, Lin, Z., Huang, Z., Peng, A., 2019a. Food Chem. 281, 57–62.
Li, L., Zheng, H., Guo, L., Qu, L., Yu, L., 2019b. Talanta 197, 68–76.
Li, Y., He, W., Peng, Q., Hou, L., He, J., Li, K., 2019c. Food Chem. 287, 55–60.
Li, Y., Zhang, L., Dang, Y., Chen, Z., Zhang, R., Li, Yingchun, 2019d. Biosens. Bioelectron. 127, 207–214.
Liang, Y., Qu, C., Yang, R., Qu, L., Li, J., 2017. Sens. Actuators, B 251, 542–550.
Lin, X.H., Aik, S.X.L., Angkasa, J., Le, Q., Chooi, K.S., Li, S.F.Y., 2018. Sens. Actuators, B 258, 228–237.
Liu, Y., Liu, J., Tang, H., Liu, J., Xu, B., Yu, F., Li, Y., 2015. Sens. Actuators, B 206, 647–652.
Liu, S., Wang, Y., Xu, W., Leng, X., Wang, H., Guo, Y., Huang, J., 2017a. Biosens. Bioelectron. 88, 181–187.
Liu, X., Ren, J., Su, L., Gao, X., Tang, Y., Ma, T., Zhu, L., Li, J., 2017b. Biosens. Bioelectron. 87, 203–208.
Liu, Y., Shen, T., Hu, L., Gong, H., Chen, C., Chen, X., Cai, C., 2017c. Sens. Actuators, B 253, 1188–1193.
Liu, Y., Hu, X., Bai, L., Jiang, Y., Qiu, J., Meng, M., Liu, Z., Ni, L., 2018. Microchim. Acta 185, 48–55.
Liu, Z., Zhang, Y., Feng, J., Han, Q., Wei, Q., 2019. Sensor. Actuator. B Chem. 287, 551–556.
Luo, Q., Yu, N., Shi, C., Wang, X., Wu, J., 2016. Talanta 161, 797–803.
Lv, M., Liu, Y., Geng, J., Kou, X., Xin, Z., Yang, D., 2018. Biosens. Bioelectron. 106, 122–128.
Maduraiveeran, G., Sasidharan, M., Ganesan, V., 2018. Biosens. Bioelectron. 103, 113–129.
Magni, R., Espina, B.H., Shah, K., Lepene, B., Mayuga, C., Douglas, T.A., Espina, V., Rucker, S., Dunlap, R., Petricoin, E.F.I., Kilavos, M.F., Poretz, D.M., Irwin, G.R., Shor, S.M., Liotta, L.A., Luchini, A., 2015. J. Transl. Med. 1–22.
Mattsson, L., Xu, J., Preininger, C., Bui, B.T.S., Haupt, K., 2018. Talanta 181, 190–196.
Motarjemi, Y., Fritz, K., 1999. Food safety 10, 325–333.
Okan, M., Duman, M., 2018. Sens. Actuators, B 256, 325–333.
Okan, M., Sari, E., Duman, M., 2017. Biosens. Bioelectron. 88, 258–264.
Poller, A.M., Spieker, E., Lieberzeit, P.A., Preininger, C., 2017. ACS Appl. Mater. Interfaces 9, 1129–1135.
Qian, K., Deng, Q., Fang, G., Wang, J., Pan, M., Wang, S., Pu, Y., 2016. Biosens. Bioelectron. 79, 359–363.
Rad, A.O., Azadbakht, A., 2019. Microchim. Acta. 186, 56–65.
Rao, H., Zhao, X., Liu, X., Zhong, J., Zhang, Z., Zou, P., Jiang, Y., Wang, X., Wang, Y., 2018. Biosens. Bioelectron. 100, 341–347.
Ren, X., Chen, L., 2015. Biosens. Bioelectron. 64, 182–188.
Rezaei, B., Boroujeni, M.K., Ensafi, A.A., 2016. Sens. Actuators, B 222, 849–856.
Roushani, M., Nezhadali, A., Jalilian, Z., 2018. Microchim. Acta 2, 551–558.
Sari, E., Üzek, R., Merkoçi, A., 2019. ACS Sens. 4, 645–653.
Sergeyeva, T., Yarynka, D., Piletska, E., Lynnik, R., Zaporozhets, O., Brovko, O., Piletsky, S., El'skaya, A., 2017. Talanta 175, 101–107.
Shalaby, A.R., 1996. Food Res. Int. 29, 675–690.
She, Y., Wang, J., 2019. Front. Chem. 7, 130–136.
Shi, X., Lu, J., Yin, H., Qiao, X., Xu, Z., 2017. Food Anal. Methods 10, 910–920.
Shirani, M.P., Rezaei, B., Ensafi, A.A., 2019. Acta Part A Mol. Biomol. Spectrosc. 210, 36–43.
Shrivastav, A.M., Mishra, S.K., Gupta, B.D., 2015. Sensors Actuators, B Chem. 212, 404–410.
Song, H., Zhang, L., Yu, F., Ye, B.C., Li, Y.C., 2016. Electrochim. Acta 208, 10–16.
Song, D., Wang, Y., Lu, X., Gao, Y., Li, Y., Gao, F., 2018. Sens. Actuators, B 267, 5–13.
Stassen, I., Burtch, N., Talin, A., Falcaro, P., Allendorf, M., Ameloot, R., 2017. Chem. Soc. Rev. 46, 3185–3241.
Sun, X., Gao, C., Zhang, L., Yan, M., Yu, J., Ge, S., 2017. Sens. Actuators, B 251, 1–8.
Sun, A., Chai, J., Xiao, T., Shi, X., Li, X., Zhao, Q., Li, D., Chen, J., 2018. Sens. Actuators, B 258, 408–414.
Sykora, S., Cumbo, A., Belliot, G., Pothier, P., Arnal, C., Dudal, Y., Corvini, P.F.X., Shahgaldian, P., 2015. Chem. Commun. 51, 2256–2258.
Tan, X., Hu, Q., Wu, J., Li, X., Li, P., Yu, H., Li, X., Lei, F., 2015a. Sens. Actuators, B 220, 216–221.
Tan, X., Wu, J., Hu, Q., Li, X., Li, P., Yu, H., Li, X., Lei, F., 2015b. Anal. Methods 7, 4786–4792.
Tang, Y., Gao, J., Liu, X., Gao, X., Ma, T., Lu, X., Li, J., 2017. Food Chem. 228, 62–69.
The´venot, D.R., Toth, K., Durst, R.A., Wilson, G.S., 2001. Pure Appl. Chem. 16, 2333–2348.
Toro, M.J.U., Marestoni, L.D., Sotomayor, M.D.T., 2015. Sens. Actuators, B 208, 299–306.
Turco, A., Corvaglia, S., Mazzotta, E., 2015. Biosens. Bioelectron. 63, 240–247.
Turco, A., Corvaglia, S., Mazzotta, E., Pompa, P.P., Malitesta, C., 2018. Sens. Actuators, B 255, 3374–3383.
Uzek, R., Sari, E., Serap, S., Denizli, A., Merkoci, A., 2019. Microchim. Acta. 186, 218–227.
Uzun, L., Turner, A.P.F., 2016. Biosens. Bioelectron. 76, 131–144.
Wackerlig, J., Lieberzeit, P.A., 2015. Sens. Actuators, B 207, 144–157.
Wang, H., Yao, S., Liu, Y., Wei, S., Su, J., Hu, G., 2017a. Biosens. Bioelectron. 87, 417–421.
Wang, Y., Gan, N., Zhou, Y., Li, T., Hu, F., Cao, Y., Chen, Y., 2017b. Biosens. Bioelectron. 97, 100–106.
Wang, Y., Rao, Z., Zhou, J., Zheng, L., Fu, L., 2019a. Biosens. Bioelectron. 132, 84–89.
Wang, Y., Xie, T., Yang, J., Lei, M., Fan, J., Meng, Z., Xue, M., Qiu, L., Qi, F., Wang, Z., 2019b. Anal. Chim. Acta 1070, 97–103.
Wei, X., Hao, T., Xu, Y., Lu, K., Li, H., Yan, Y., Zhou, Z., 2016. Sens. Actuators, B 224, 315–324.
Wei, Y., Zeng, Q., Wang, M., Huang, J., Guo, X., Wang, L., 2019. Biosens. Bioelectron 131, 156–162.
Wu, S., Zhang, H., Shi, Z., Duan, N., Fang, C., Dai, S., Wang, Z., 2015. Food Control 50, 597–604.
Wu, L., Lin, Z., Zhong, H., Peng, A., Chen, X., Huang, Z., 2017a. Food Chem. 229, 847–853.
Wu, L., Lin, Z., Zhong, H., Chen, X., Huang, Z., 2017b. Sens. Actuators, B 239, 69–75.
Wu, Y., Tilley, R.D., Gooding, J.J., 2018. J. Am. Chem. Soc. 141, 1162–1170.
Xiao, T.T., Shi, X.Z., Jiao, H.F., Sun, A.L., Ding, H., Zhang, R.R., Pan, D.D., Li, D.X., Chen, J., 2016. Biosens. Bioelectron. 75, 34–40.
Xiao, L., Zhang, Z., Wu, C., Han, L., Zhang, H., 2017. Food Chem. 221, 82–86.
Xu, S., Lu, H., 2015. Biosens. Bioelectron. 73, 160–166.
Xu, L., Fang, G., Pan, M., Wang, X., Wang, S., 2016. Biosens. Bioelectron. 77, 950–956.
Xu, S., Lin, G., Zhao, W., Wu, Q., Luo, J., Wei, W., Liu, X., Zhu, Y., 2018. ACS Appl. Mater. Interfaces 10, 24850–24859.
Yan, Z., Gan, N., Li, T., Cao, Y., Chen, Y., 2016. Biosens. Bioelectron. 78, 51–57.
Yang, J.C., Park, J.Y., 2016. ACS Appl. Mater. Interfaces 8, 7381–7389.
Yang, G., Zhao, F., 2015. Sens. Actuators, B 220, 1017–1022.
Yang, Y., Niu, H., Zhang, H., 2016. ACS Appl. Mater. Interfaces 8, 15741–15749.
Yang, B., Gong, H., Chen, C., Chen, X., Cai, C., 2017. Biosens. Bioelectron. 87, 679–685.
Yao, T., Gu, X., Li, T., Li, J., Li, J., Zhao, Z., Wang, J., Qin, Y., She, Y., 2016. Biosens. Bioelectron. 75, 96–100.
Yin, W., Wu, L., Ding, F., Li, Q., Wang, P., Li, J., Lu, Z., Han, H., 2018a. Sens. Actuators, B 258, 566–573.
Yin, Z.Z., Cheng, S.W., Xu, L.B., Liu, H.Y., Huang, K., Li, L., Zhai, Y.Y., Zeng, Y.B., Liu, H.Q., Shao, Y., Zhang, Z.L., Lu, Y.X., 2018b. Biosens. Bioelectron. 100, 565–570.
Yılmaz, E., Ozgur, E., Bereli, N., Turkmen, D., Denizli, A., 2017. Mater. Sci. Eng. C 73, 603–610.
Yue, X., Luo, X., Zhou, Z., Bai, Y., 2019. Food Chem. 289, 84–94.
Zamora-Gálvez, A., Mayorga-Matinez, C.C., Parolo, C., Pons, J., Merkoçi, A., 2017. Electrochem. Commun. 82, 6–11.
Zhao, X., Hu, W., Wang, Y., Zhu, L., Yang, L., Sha, Z., Zhang, J., 2018. Carbon 127, 618–626.
Zheng, L., Zhang, C., Ma, J., Hong, S., She, Y., Ei-aty, A.M.A., He, Y., Yu, H., Liu, H., Wang, J., 2018. Anal. Biochem. 559, 44–50.
Zhang, F., Luo, L., Gong, H., Chen, C., Cai, C., 2018. RSC Adv. 8, 32262–32268.